HAL open science

Converting carbon vulnerable lands to wood plantations for use as building materials: overall environmental performance and time-dependent assessment of carbon dioxide removals

Zhou Shen, Lorie Hamelin, Ligia Tiruta-Barna

▶ **To cite this version:**

Zhou Shen, Lorie Hamelin, Ligia Tiruta-Barna. Converting carbon vulnerable lands to wood plantations for use as building materials: overall environmental performance and time-dependent assessment of carbon dioxide removals. Journal of Cleaner Production, 2023, 388, pp.136040. 10.1016/j.jclepro.2023.136040 . hal-04335081

HAL Id: hal-04335081

https://hal.science/hal-04335081v1

Submitted on 11 Dec 2023

HAL is a multi-disciplinary open access archive for the deposit and dissemination of scientific research documents, whether they are published or not. The documents may come from teaching and research institutions in France or abroad, or from public or private research centers.

L'archive ouverte pluridisciplinaire **HAL**, est destinée au dépôt et à la diffusion de documents scientifiques de niveau recherche, publiés ou non, émanant des établissements d'enseignement et de recherche français ou étrangers, des laboratoires publics ou privés.

Converting carbon vulnerable lands to wood plantations for use as building materials: overall environmental performance and time-dependent assessment of carbon dioxide removals.

Zhou Shen, Lorie Hamelin, Ligia Tiruta-Barna*

TBI, Université de Toulouse, CNRS, INRAE, INSA, Toulouse, France

* corresponding author

Abstract

Bioeconomy addresses the triple balancing challenge posed by the Paris Agreement: inducing additional GHG mitigation alongside biophysical carbon dioxide removals, while keeping fossil carbon in the ground. The use of woody plants as construction materials could simultaneously address this challenge: CO_2 is absorbed through photosynthesis, while wood-based products provide mitigation by replacing either petrochemical materials such as plastic boards or energy-intensive materials like bricks. This study combines, at the scale of France, static and dynamic life cycle assessment with soil carbon simulations to investigate the long-term environmental performance of using, as input for the building sector, black locust (*Robinia pseudoacacia* L.) planted on "carbon vulnerable lands". These are areas specifically selected for their low soil organic carbon (SOC) levels and low potential to interfere with food security. After the consecutive cultivation of three rotations, black locust was shown to stock an additional 92000 kg ha^{-1} of carbon in soils as SOC. The mitigation effect from the plastic board replacement is the major contributor to the assessed environmental impacts, including climate change, leading the black locust system to generally perform better than the reference system where the carbon vulnerable areas are left as they are with their initial vegetation. Considering that cultivation starts in 2022, the dynamic evaluation of the global mean temperature change (GMTC) shows that the black locust system results in net negative emissions in the near- and mid-term, but with a GMTC overshot in the second half of the century. Even if a considerable carbon stock is created through time (e.g., 81% and 39% of the carbon captured by photosynthesis, in 2050 and 2100 respectively), the GHG emissions stemming from manufacturing and end-of-life processes were shown to offset the benefit of carbon capture.

Keywords: soil organic carbon, consequential life cycle assessment, dynamic life cycle assessment, climate change mitigation, biomass, negative emissions

Graphical abstract (see figures document)

Highlights:

- Black locust plantation and utilization in buildings induce negative emissions
- Black locust system yields greater climate benefits than the initial vegetation
- Plastic board replacement explains the superior performance for 13/16 impacts
- By 2136, the largest temperature reduction of 3.9E-09 K per ha is simulated
- 15% of the carbon captured by 3 rotations is still stocked after 260 years

List of Abbreviations

A	radiative efficiency of a GHG
B	atmospheric burden of a GHG
BL	black locust scenario
BLc	black locust scenario evaluated by consequential LCA
BLa	black locust scenario evaluated by attributional LCA
C	carbon
CLT	cross-laminated timber
CO_2	carbon dioxide
CSAAP	carbon Storage in Arable land and Anthropogenic Products
CV-land	carbon vulnerable land
FU	functional unit
g	emission flow of a GHG
GHG	greenhouse gas
GMTC	global mean temperature change
iLUC	indirect land use chanage
IRF	concentration - impulse response function of a GHG
IRFT	temperature – impulse response function
LCA	life cycle assessment
MDF	medium density fiberboard
REF	reference scenario
REFc	reference scenario evaluated by consequentnial LCA
REFa	reference scenario evaluated by attributional LCA
RF	radiative forcing
SOC	soil organic carbon

SM	supplement information material
t	metric ton
y	year

1. Introduction

Achieving the climate objectives of the Paris Agreement and national policies in terms of emissions reduction and carbon neutrality by 2050 implies the implementation of drastic greenhouse gas (GHG) emission reductions and carbon dioxide (CO_2) capture and storage actions. To this end, the concept of Carbon Storage in Arable land and Anthropogenic Products (CSAAP) has recently been proposed (Shen et al., 2022b), consisting in cultivating plants, also called biopumps, that can induce a net increase of soil organic carbon (SOC) stocks while providing biomass for long-lasting anthropogenic products.

Putting CSAAP into practice needs solving two issues, namely defining the type of suitable biopump species and areas to grow them. According to previous research (Shen et al., 2022b), there are up to 2,400,000 ha of suitable land in France alone that could be available for planting biopumps for climate mitigation purposes. These lands are called 'carbon vulnerable lands (CV-lands)' as they present a high potential for SOC sequestration due to their current SOC stock being <50 t C ha^{-1} (Minasny et al., 2017). They were also selected to respect a set of specific sustainability criteria defined in Shen et al. (2022b). Among the list of 14 suitable woody biopumps presented in Shen et al.(2022b), black locust *(Robinia pseudoacacia* L.) was highlighted not only because it could capture 31.5 kg CO_2 per tree per year (Supplementary material, SM, section 2.1), but also for its capacity to convert part of the captured C in the soil as SOC (Wang et al., 2012). Furthermore, woody products have a relatively long lifetime, hence

delaying the return of C to atmosphere as gaseous emissions (CO_2, and eventually methane and carbon monoxide) .

When analyzing how wood value chains affect climate change, the conventional theory considers biogenic CO_2 as neutral (balanced), thus neither CO_2 absorbed nor CO_2 emitted from biomass is included in climate change impact calculations (Chen et al., 2019; da Costa et al., 2018). This approach is suitable for annual or short rotation coppice, while not proper in estimating forest mitigation potential because the effect of C storage and delayed emission is ignored. Guest et al. (2013) studied the relationship between the wood rotation and C storage in products on the biogenic global warming potential. They concluded that in order to consider biogenic CO_2 as neutral, the lifespan of wood products should be at least half of the plantation rotation. Another common accounting approach is considering the forest as a permanent C sink, where the CO_2 captured through photosynthesis is counted while the emission of biogenic CO_2 is not (González-García et al., 2011). This approach shows the effectiveness of biomass as a C sink on a limited time scale, however, it is not correct under time scales encompassing the life cycle of biomass from cradle-to-grave. Albers et al. (2019b) modeled the trees' growth and residue decomposition, showing that the tree's lifetime highly influences the mitigation potential, the shorter the lifetime, the lower the mitigation effect of converting forests to biofuels. However, since biofuels are used at once with almost all C emitted immediately, there is no technosphere C sink. Lan et al. (2020) tracked the carbon flows from one rotation of pine forest cultivation to the end of wood products on a 100-year scale, and highlighted the difference between using residue for wood products or energy. They treated biogenic CO_2 as neutral, only considering the influence of fossil CO_2 emissions. Zieger et al. (2020) counted both biogenic CO_2 absorption by timber and wheat, and degradation of biobased walls including incineration and compost, in a time-dependant manner. However, the belowground part of plants and the SOC changes were not included in these studies. Soil is an important C sink, not

taking it into account results in C flows that are not correctly balanced (Hamelin et al., 2012). Moreover, because aerial crops are commonly harvested, soil and root carbon storage is a key determinant of climate change mitigation potential, and tends to be higher with greater plant diversity, according to experimental results (Yang and Tilman, 2020).

The most existing LCA studies use a static approach and CO_2-eq as an aggregation metric for all GHG, independently of the time scale considered, which could mislead the conclusions (Barna, 2021; Saez de Bikuña et al., 2018; Zieger et al., 2020). Because wood and wood-based products have a relatively long lifespan, and biomass residues decay at different rates, the temporal factor is essential in assessing wood product systems. Recent studies demonstrated a considerable difference between static and dynamic LCA approaches for wood-based products (e.g., Cardellini et al., 2018; Göswein et al., 2020), especially for the quantification of biogenic CO_2 capture and release effects. A recent study pointed out that for woody products, the static LCA overestimates the long-term cumulative impact without providing information on short-term impact (Cordier et al., 2022). Although the study built the results on a temporal inventory of C flows, the climate change impact was calculated by a metric based on CO_2-eq which induces a bias in the results.

This work explores the mitigation potential for global warming and for overall environmental impacts, of an application case of the CSAAP strategy with perennial plantations, selected in the light of earlier work (Shen Zhou; Ligia Tiruta-Barna Shivesh Kishore Karan; Lorie Hamelin, 2022). The case is the implementation of a 35-y plantation of black locust on CV-lands in France, using the biomass for bio-based products intended for the building sector. Objectives are to: 1) evaluate the C sinks induced over time, 2) investigate the overall environmental consequences of replacing current CV-land and fossil-based products with the black locust system and the related bio-based products, and particularly the global warming mitigation potential in order to contrast it with the sinks, and 3) investigate the effect on global

mean temperature change in time. In the general endeavor to uncover environmentally-performant solutions towards both carbon dioxide removals and GHG mitigation, this work proposes an original, comprehensive framework with adapted modeling tools to address all these objectives, and to fill gaps in the existing literature. The C flows were modeled from the tree cultivation to products manufacturing and end of life (for a cradle-to-grave scope), and the C pools in soil (SOC) and materials (biomass) were estimated in function of time. The time period encompasses the tree cultivation (three rotations) but also the product lifetime and end of life period with slow material degradation. The dynamic C balance, but also all GHG temporal emissions over the life cycle were integrated in dynamic LCA for global warming impact, evaluated by the global mean temperature change indicator. The overall environmental consequences of changing the initial land use to black locust cultivation and utilization were evaluated with the consequential LCA approach. Finally, sensitivity and uncertainty analysis were performed to explore the robustness of the results obtained.

2. Methods

2.1. Scenarios description

The point of departure of this analysis is one hectare of average French CV-land, to be either converted for black locust cultivation from the year 2022, over three rotations of 35-y each (BL Scenario), or maintained as CV-land for 105 y (reference scenario, from here onwards referred to as REF Scenario). For the static environmental assessment, only 35 years (the time of one rotation) is considered, as further detailed in section 2.5.

2.1.1 Initial vegetation scenario on CV-land (REF Scenario)

This scenario considers that CV-lands remain CV-lands throughout the time covered by the analysis. The vegetation considered on average French CV-land stem from the work of (Shen et al., 2022; Shen Zhou; Ligia Tiruta-Barna Shivesh Kishore Karan; Lorie Hamelin, 2022). Accordingly, four types of initial land cover are considered with different shares in terms of the area they cover, namely intensive grasslands (53%), natural grasslands (20%), rapeseed lands (20%), and woody moorlands (7%) (details in Shen et al., 2022b). Ryegrass (*Lolium perenne* L.) and rapeseed (*Brassica napus* L.) represent the initial vegetation on intensive grassland and rapeseed lands, respectively, while heather (*Calluna vulgaris*) is selected to represent both natural grasslands and woody moorlands vegetation. On CV-lands remaining CV-lands, ryegrass and rapeseed are harvested annually and used for animal feed and oil production respectively, while heather is considered to decay on-site (Pehme et al., 2017). The rapeseed cake co-produced with rapeseed oil is also considered to be used for animal feed.

2.1.2 Black locust scenario (BL)

In this scenario, CV-lands are ploughed prior to black locust planting. Black locust is a nitrogen-fixing species and tolerates droughts (Nicolescu et al., 2020; Seserman et al., 2018). For this reason, and also in accordance with the CSAAP vision to favor systems with minimal inputs (Shen et al., 2022), no fertilization or irrigation is considered. To remove defective trees, selective thinning is conducted twice, in the 10th year and 20th year of the plantation's lifetime, where whole trees are removed (Keresztesi, 1983; Nicolescu et al., 2020). After the second selective thinning, extra branches are pruned to provide enough space for stem growth. After harvesting, black locust is delimbed and debarked. Barks are incinerated to provide heat for downstream manufacture (Silva et al., 2013), while branches are chopped into wood chips (Fig. 1a). Stumps are crushed and left on the ground as residues during thinning operations when black locust is logged.

The processes after logging are depicted in Fig. 1b. First, there is the processing of stems. After delimbing and debarking, the stems are dried on open fields to meet a moisture content of ca. 15% (Żelazna et al., 2019). The dried stems are trimmed and sawn into panels, then laminated into several layers (Sahoo et al., 2019). These high-value laminated panels, called 'cross-laminated timber' (CLT), are widely used in the building sector, as a more sustainable alternative than carbon-intensive materials (Cadorel and Crawford, 2019; Cowie et al., 2021). Herein CLT is assumed to be used for exterior walls, with 50 years lifespan (Dodoo et al., 2014). After demolition, 45% of CLT is incinerated, 45% is recycled, while the remaining 10% is lost (regarded as open-landfills) (Jayalath et al., 2020). The recycled CLT is chopped into wood chips for further treatment.

Second, the branches from stem's trimming are cut into chips (to produce medium density fiberboard, MDF), then wood chips are washed to remove the dust. The clean chips are mixed with other wood chips obtained from branches, along with the woody material from 1st and 2nd thinning and recycled CLT. All these materials are softened in a steam-pressurized digester (the heat to generate steam commonly comes from burning barks), then mixed with urea-formaldehyde resin and additives in the resonating process, to improve the strength (Puettmann et al., 2016). The mixture is pressed into boards (MDF) at 170 °C for ca. 5 minutes using a mechanically controlled oil-heated press (Yuan and Guo, 2017). The produced MDF has multiple usages. Having a lower mechanical strength than CLT, it is more suitable for furniture and interior architecture (Piekarski et al., 2017). After 12 years of use, most MDF in Europe is incinerated with heat recovery, while a minor part is landfilled (Couret et al., 2017; ecoinvent, 2020). The scraps occurring through the MDF production process are considered to end in open-landfills.

Fig. 1 Process flow diagram showing the key activities considered for (a) black locust cultivation, harvesting (green) and residual biomass management (orange), and (b) manufacture and disposal of cross-laminated timber (CLT; yellow) and medium density fiberboard (MDF; blue).

2.2. Overview of the methodology used

The methodology used to achieve the objectives of this study builds on material and energy flow calculation, encompassing all stages from plant cultivation to anthropogenic production and products' end of life, to finally evaluate the carbon pools and environmental impacts.

Fig. 2 Calculation steps followed in this study

As shown in Fig. 2, the first step calculates the growth of black locust to determine how much CO_2 is captured by photosynthesis, how much biomass is produced in function of time in the different parts of the plant (e.g., belowground, aboveground), and the quantity of residues destined to decay above- and below ground. The carbon in the residues is an input to a SOC model, whose evolution is simulated over the rotation time span. In this way, the yearly content of SOC is estimated (over 105 years), along with the CO_2 releases from mineralization or native SOC losses, as detailed in section 2.4. The harvested biomass enters the manufacturing chains and determines the amount of products, associated by-products, and all related flows in the process chain, from harvesting to product manufacturing and end of life. Data from literature have been used to model the material and energy balances for the manufacturing processes.

These foreground flows are then used in three different LCA modeling approaches to respond to different questions as later detailed: static consequential LCA, dynamic LCA using

the same consequential modeling of the inventory, and dynamic LCA using the attributional modelling of the background inventory with system expansion in the foreground part. For the dynamic approaches, the material and energy flows have been used as time series with their time occurrence depending on the system's timeline. Both dynamic approaches used temporal predictions for electricity mix (used in the background inventory) based on either the absolute values or the rate of changes.

2.3 Black locust growth rate

Black locust is a fast-growing tree species. After seedling planting, it reaches its fastest growth rate at year 20, then the growth rate slows down gradually till the end of the rotation (year 35) (Ciccarese et al., 2014; Nicolescu et al., 2018). The volume of biomass is estimated from the height and diameter at breast height, calculated in function of time (Rédei et al., 2014, 2012). The wood volume is converted to biomass dry matter considering a wood density of 785 kg m^{-3} DM (Adamopoulos et al., 2007) (SM 2.2).

The whole stand is assumed to grow at the same rate, thus the below-ground biomass is calculated based on a fixed shoot/ root ratio in time, here taken to 1.73 (Chen et al., 2020). In order to calculate the biomass amount per ha in a specific year, a density varying between 560–2240 trees per ha is considered, according to the growth stage (Keresztesi, 1983; Nicolescu et al., 2018). Details and results of simulated annual biomass partition (above- and below ground; in standing biomass and residues; as woody and non-woody portions) are presented in SM 2.2.

The foliage, pods, and seeds are considered jointly under the umbrella term 'aerial biomass', and are regarded as an annual input to soils from the 6th year of the rotation (Stone, 2009; Warne, 2016). Similar to the root biomass, the aerial biomass increase in time with the tree growth (Ciccarese et al., 2014). It was estimated based on a fixed ratio (1.2% of wood biomass, DM).

2.4 Simulating SOC on CV-lands for both scenarios, and wood residues decay

The evolution of SOC on CV-lands cultivated with black locust or covered with initial vegetation was simulated with C-TOOL (Taghizadeh-Toosi et al., 2014). This model was adopted as one of the few models easily usable (i) with unconventional (non-agricultural) crops, (ii) for perennial systems, and (iii) calibrated for temperate areas (Andrade et al., 2022). Among others, it has the advantage that the proportion of C incorporated in the different (virtual) soil pools (each with a different turnover rate affected by clay content and temperature; C-TOOL considers three pools) is easily customizable (e.g., Hansen et al., 2020). This ease of customization also applies to the allometric equations used to define the proportion of aboveground residual biomass input to the soil annually. Different applications of the model with perennial crops include (Hamelin et al., 2012) and (Keel et al., 2017).

The simulation was conducted with a one-year time step, for a timespan of 105 years from 2022 to 2126, corresponding to three consecutive rotations of black locust. Meteorological conditions in France were predicted by SICLIMA (DRIAS CERFACS, IPSL, last updated May 2013) for the RCP4.5 climate trajectory (Representative Concentration Pathway; Chen et al., 2021), downscaled by the model CNRM-CERFACS-CM5/CNRM-ALADIN63. In C-TOOL, only the monthly average temperature is required in terms of meteorological data input (Fig. s1). The required soil characteristics include the soil clay content and the C/N ratio. The former was retrieved from the same database used for identifying CV-lands (GSOC; Food and Agriculture Organization of the United Nations, 2020), the latter, not included in GSOC, was set to 11 based on relevant literature (Clivot et al., 2019; Launay et al., 2021). The average initial SOC content for the CV-lands was evaluated as 42350 kg SOC ha^{-1} (Shen et al., 2022).

Finally, one other key input required by the model is the annual C input from residual above- and belowground biomass. The aboveground resides includes aerial biomass (foliage, seeds, and pods), which fall down annually (except for the first five years), and stumps, which

are crushed and left on the ground as residues during thinning operations and when black locust is logged (year 10th, 20th, 35th of the rotation, respectively). Belowground residues consist of decaying roots and rhizodeposits. Decomposition rate coefficients of 0.12, 0.008, and 0.003 months^{-1} were set for aerial, aboveground- and belowground wood biomass, respectively (Taghizadeh-Toosi et al., 2014). To represent the slower decay of woody above- and below-ground residues, the simulation was conducted for an additional 100 years after the last rotation (the C not emitted after 100 years is considered as permanently stored).

For the initial vegetation, consisting of four different land types, the SOC of each land type was simulated individually, then aggregated together based on their respective shares in 1 ha CV-land (C input in Table s19). A decomposition rate coefficient of 0.12 month^{-1} was used for the initial vegetation' residual biomass inputs to soil (above- and below-ground), as used for the foliage and as used in e.g., Hamelin et al. (2012) and Taghizadeh-Toosi et al. (2014) (both on the basis of Petersen et al., 2005).

2.5 Environmental impact assessment through consequential LCA

2.5.1 Goal, boundary, and functional unit

Consequential LCA is used to evaluate the environmental consequences of (i) cultivating black locust instead of the initial vegetation on the identified CV-lands in France and (ii) using the biomass in anthropogenic products while replacing conventional (fossil-based) products. This implies that multifunctionality was modeled with system expansion (Fig. 3) and that the life cycle inventories for marginal suppliers were considered. The functional unit is defined as 'using 1 ha of CV-land in France for cultivating perennial crops over one full rotation, and using the harvestable biomass within the bioeconomy'. For the scenarios considered herein, this implies 35 years. The LCA framework follows the ISO 14040 and 14044 standards (ISO,

2006a, 2006b). The system boundary considered for the consequential LCA is shown in Fig. 3, both for the BL (here BLc) and REF (here REFc) scenarios.

Fig. 3 System diagrams showing the boundaries considered in consequential LCA of business as usual (REFc) and black locust (BLc) systems, built on REF and BL scenarios respectively. CV-land: carbon vulnerable land; iLUC: Indirect land use changes; CLT: cross-laminated timber; MDF: medium density fiberboard. Full lines indicate induced processes while dotted lines represent avoided processes.

System BLc involves a variety of substitutions. The vegetable oil (rapeseed oil) and feed (ryegrass silage, rapeseed cake), no longer reaching markets because CV-lands are now used for black locust have to be compensated for (Saez de Bikuña et al., 2018). This may happen through two main reactions, namely expansion of nature for agriculture (deforestation) or intensification of agricultural land (Tonini et al., 2016), both considered herein under the umbrella term of indirect land use changes (iLUC). According to market reports and literature review, the bio-based CLT and MDF will replace light-clay bricks and polyvinyl-chloride boards (herein referenced as plastic boards), respectively (Onyeaju et al., 2012; Takano et al., 2014). Incineration, at all stages where it happens, is considered with heat recovery, which implies that this heat will not need to be generated the way it would have otherwise been. As a result, corresponding heat generation is avoided. Finally, the use of CLT at the expense of bricks (replaced material) was considered to lead to a 52% reduction of the electricity consumed in the erection and demolition phases, because of the lighter mass (Corradini et al., 2019; Guo et al., 2017).

2.5.2 Life cycle inventory

349 Life cycle inventories for foreground processes (Fig. 1) were established on the basis of
350 literature, models, and a variety of estimation proxies when necessary. These are
351 comprehensively detailed in the SM (Tables s3-s18). The displaced feed service (for the silage
352 ryegrass and rapeseed cake of the initial vegetation) and its substitution by corresponding
353 marginal carbohydrates, protein and lipid ingredients, along with the associated land use
354 changes were modelled according to the methodology described in (Tonini et al., 2016).
355 Landfilling processes (open-landfilling and landfilling of MDF at the end-of-life) were
356 modelled according to the model provided in IPCC (2019), which proposes a time-dependant
357 decay function, and that C emissions arise as 14% CH_4-C, and 86% CO_2-C. According to the
358 IPCC (2019) landfilling model, 15% of the products' biogenic C is considered to end as
359 emissions to air. For the static LCA, the overall SOC change simulated with C-TOOL was, for
360 both systems (BLc and REFc), annualized (i.e. distributed equally) over the 35 years of the
361 rotation. All the background inventories were taken from Ecoinvent v3.5 (ecoinvent, 2020),
362 with the consequential model.
363

364 **2.5.3 Life cycle impact assessment and interpretation**

365 The environmental impact assessment was performed with the Environmental Footprint
366 method (EF) recommended by European Commision (Fazio et al., 2018a). Moreover, because
367 all CO_2 releases and adsorption are accounted, biogenic CO_2 was considered with a global
368 warming potential of 1 kg of CO_2-eq per kg biogenic CO_2 instead of the value of 0 used in
369 (Fazio et al., 2018a).

370 For interpretation, a contribution analysis was performed for each impact category,
371 where processes with negative and positive contributions were analyzed separately in two
372 groups. In each group, the processes contributing to at least 80% of the impact were selected
373 for further in-depth analysis, i.e., identifying their sub-processes and substances contributing to

the impact (Fazio et al., 2018b). The LCA was facilitated with the SimaPro software, version 9.1.

2.6 Dynamic LCA for evaluating climate change impact

Given the long lifetime of the studied system, a time-dependent method is necessary to address the temporal dimension of the climate change impact. Dynamic LCA with the global mean temperature change (GMTC) as an indicator was applied herein. The method and computational tool used were presented in previous works (Tiruta-Barna, 2021; CCI-tool, 2021). The GMTC calculation used the recommended method of IPCC, for the emission timing over the whole life cycle of scenarios (Stocker et al., 2013), for all GHGs included in the ecoinvent v3.5 database (Table s21), and can be summarized by the following main equations.

The atmospheric burden of substance s, B_s (kg), is calculated as the convolution product (symbol $*$) between the temporal emissions of the substance, g_s (kg.year^{-1}), and the concentration - impulse response function of that substance, IRF_s :

$$B_s(t) = g_s * IRF_s = \int_0^t g_s\left(t'\right) IRF_s\left(t - t'\right) dt' \quad (1)$$

where t and t' are two time scales. The radiative forcing RF is calculated by:

$$RF_s(t) = A_s(t)\, B_s(t) = A_s(t)(g_s * IRF_s) \quad (1)$$

where A_s (W.m^{-2}.kg^{-1}) is the radiative efficiency (considered as constant). IRF and A are specific for each GHG (Stocker et al., 2013). The global mean temperature change generated by the forcer s is defined as the convolution product between its RF and the temperature impulse response function IRFT:

$$GMTC_s(t) = RF_s * IRFT_s \quad (3)$$

IRFT is independent of the type of GHG. The mean temperature change at a given time t, GMTC (K), is obtained by aggregating values for all the concerned forcers:

$$\mathrm{GMTC(t)} = \sum_s \mathrm{GMTC_s(t)} \quad (4)$$

In scenario BL, trees are cultivated on 1 ha of land for three consecutive rotations, from 2022 to 2126. The same time span is considered for the initial vegetation lasting on the CV-lands in scenario REF. The temporal inventory (limited herein to GHGs) was obtained by placing each process on the timeline shown in Fig. 4. For long-lasting biogenic GHG emissions (e.g., those stemming from the disposal of CLT and MDF), the longest emission time was set as 100 years because the C released after 100 years can be considered permanently stored (European Commission-Joint Research Centre., 2010). Therefore, the temporal scope spans over the implantation of the first rotation in 2022, up to the end of the emissions, in 2290, from the last MDF disposal, covering 267 years in total. The manufacturing processes were considered to occur in the year of biomass harvesting. The time step for the inventory calculation was set to 1 year, regarded as sufficiently fine for climate change impact calculation.

Two perspectives were adopted for the dynamic modeling, here referred to 'consequential' and 'attributional', despite not fully embracing all features attributed to these two types of modeling approaches (Brandao et al., 2017; Schaubroeck et al., 2021). These two perspectives imply two main differences. One is the system boundary, as illustrated in Fig. 3 for the consequential perspective and Fig.5 for the attributional perspective. Both perspectives compare the black locust system to a reference situation. In the consequential perspective, the system expansion reactions (associated with both the products generated in the BL system and the consequences of the foregone use of CV-land) are placed in the BL system (or here BLc). Even the foregone use of CV-land (emissions associated with growing ryegrass, rapeseed, and heather) could have been placed in this system for an entirely relative perspective, it was left as

421 a reference (here REFc) for comparison purposes. Two realities are compared in what is here
422 referred to as "attributional perspective". In one (BLa), black locust is grown on CV-land and
423 used to produce heat, CLT, MDF (the latter two being in use for a number of years and disposed
424 of at their end-of-life, the same way as in the BLc system), while vegetable oil is supplied by
425 palm oil and feed by marginal feed ingredients. In the other system (REFa), CV-land is used as
426 CV-land, but to make it equivalent, the alternatives to products generated in the BLa system
427 (heat, bricks, plastic boards) are considered here. Strictly speaking, these two system boundaries
428 are equivalent (and would typically be both labelled as "consequential"). The major difference
429 between the two perspectives lies in the type of background data being used. The consequential
430 perspective considered marginal data, e.g., those foreseen to react to a demand change in the
431 long-term (concretely translating in the use of the so-called consequential background
432 processes), while the attributional perspective used average background data (cut-off processes).
433 Moreover, for the foreground data requiring heat and electricity, the attributional perspective
434 considered the mix composition predictions made for France for different periods (2020-2030,
435 2030-2040, 2040-2050), based on Kassara et al. (2019) for electricity and (ADEME, 2018) for
436 heat. The heat and electricity mixes after 2050 were considered the same as in 2050 (Table s22-
437 24). For the consequential perspective, the marginal French electricity mix of Ecoinvent v3.5
438 was considered (2050; based on predictions from (European Commission, 2021)). For
439 foreground heat, natural gas is considered.
440
441 Fig. 4 Timeline of processes for dynamic LCA.
442
443 Fig. 5 System diagrams of business as usual (REFa) and black locust (BLa) systems, built on
444 REF and BL scenarios respectively.
445

446 **2.7 Sensitivity and uncertainty analysis**

447 To explore the robustness of the obtained results and identify the hotspots, sensitivity
448 and uncertainty analysis were conducted for both scenario BLc and REFc. The method and
449 results are described in SM 5 and 6, for the sensitivity and uncertainty of the systems,
450 respectively.

451

452 **3 Results and discussion**

453 **3.1 Black locust growth and decay**

454 Based on simulated height and diameter (Fig. s5), the biomass amount on 1 ha CV-land
455 is shown in Fig. 6a, in different parts of black locust. During each thinning operation (year 10
456 and 20), half of the tree (in terms of dry matter, DM) is logged, in year 10 and 20, producing
457 26 and 110 t of woody DM respectively, being further chipped to produce MDF. The final
458 harvesting at year 35 produces 368 t DM of stem (which is used to produce CLT), and 136 t
459 DM of branches used for MDF. Based on the different turnover rate simulated by C-TOOL, 10%
460 and 27% of the DM in above- and belowground wood residues is still undegraded after 35 years.
461 This falls to 1.5% and 2.8% after 100 years of decomposition.

462

463 **3.2 SOC simulation results**

464 The simulation results with C-TOOL (Fig. 6b) shows that SOC increased at the end of
465 the rotation with black locust while slightly decreased with the initial vegetation. The black
466 locust induces a SOC increase periodically with each rotation, reaching 92040 kg ha^{-1} at the
467 end of the third rotation (year 2126). The greatest increase is observed during the first rotation
468 with 73650 kg ha^{-1}. The SOC increase is less important for the subsequent rotations, being only
469 15540 and 2840 kg ha^{-1} for the second and third rotation respectively, since the SOC gradually

470 reaches saturation in soils (Petersen et al., 2013). Declining SOC stocks are observed following
471 every biomass removal event (harvest, thinning) due to lesser input into the soil.

472 Unlike the black locust system, the SOC in the initial vegetation system decreased from
473 42350 to 40680 kg ha^{-1} during the cultivation (105 years). The main difference between black
474 locust and initial vegetation is the C input. According to the literature data for vegetation yield
475 and to the simulation results for black locust growth, the aboveground C inputs from initial
476 vegetation is higher than that from black locust aerial biomass (foliage, seeds and pods) (1.27
477 and 0.91 t ha^{-1} $year^{-1}$ respectively). The higher C input implies that a greater quantity of C is
478 humified; as a result, the SOC of the initial vegetation is higher than black locust until year
479 2031. But at years 10, 20, and 35 of the rotation, there are extra C inputs from logged stems,
480 especially from the belowground root portion (below-ground: 4.65, 19.23, 65.24 t C ha^{-1} from
481 the first-, second thinning, and harvesting respectively), making the SOC of the black locust
482 system being higher than the one of the initial vegetation. Meanwhile, compared to the initial
483 vegetation residues, the gradual decomposition of black locust residues keep the C in the soils
484 for a longer time, leading to the SOC of black locust exceeding the SOC of the initial vegetation
485 system by year 2041 (second thinning).

486

487 Fig. 6 Simulated (a) biomass growth and decay for black locust during one rotation, and (b)
488 SOC evolution for black locust and initial vegetation during the cultivation period.
489 Harvestable biomass: stem, branch and bark.

490

491 Considering the 105 years studied herein, an annual SOC increase of 880 kg ha^{-1} is
492 observed for the black locust system, corresponding to an increase rate of 21‰ per year, which
493 can be compared to the 4‰ target reported by Minasny et al. (2017) to offset the global annual
494 GHG emissions. Looking at each rotation in isolation, this yearly increase rate is 50‰ during

the first rotation and 30‰ during the first-two rotations, indicating that short-term cultivation might be more efficient. Ciccarese et al. (2014) simulated one rotation of black locust with the Yasso model, and observed an annual SOC increase of 110 kg ha^{-1} $year^{-1}$ before the final harvestwhich is half of our result (220 kg ha^{-1} $year^{-1}$ for the first rotation). On the other hand, Wang et al. (2015) reported, based on field measurements, an average annual SOC increase of 930 kg ha^{-1} (over 25 years). They measured this increase to 2200 kg ha^{-1} annually from year 5-10 but only 290 kg ha^{-1} from year 10-25. Both studies also highlighted the contribution of dead wood incorporated in soils.

It should be noticed that the high SOC at the end of harvesting does not last for a long time. Fig. s2 shows that following the last stem harvest, the SOC decreases gradually since there is no extra C input anymore. After 51 years (2177) and under the conservative assumption that the soil is left bare, all SOC gained with the black locust cultivation is lost, the SOC stock being equivalent to the initial level of 2022.

3.3 Environmental impact results from the static LCA

The LCA results are shown in Fig. 7 (climate impact; global warming potential for a 100-y time horizon, GWP_{100}) and Fig. 8 (all other impacts); the negative contributions represent avoided processes or emissions while positive contributions represent the processes induced by implementing the studied scenario. The difference between these represents the net impact of a given category and scenario. Results are expressed per functional unit.

3.3.1 Climate change

Both scenarios lead to a negative characterized impact for climate change, but scenario BLc leads to a larger magnitude than scenario REFc (-2202 vs -51 t CO_2-eq). In scenario BLc (Fig. 1a), the tree cultivation and the avoided plastic boards processes shape the

net negative score, respectively contributing with -1283 and -2509 t CO_2-eq. The material substitution contributes the most to negative restuls, which is also observed in a recent LCA study on woody products (Cordier et al., 2022). The avoided plastic board process is an aggregation of several activities. About 61% of its impact is due to petrochemical plastic manufacture, while 24% stems from incineration at the end-of-life (Fig. s4). The negative score of tree cultivation reflects the net 1305 t CO_2 captured by black locust in one rotation, offsetting the positive GHG emission due to the iLUC in the same process (21 t CO_2-eq).

On the other hand, emissions during the biomass logging (combining harvesting, thinning and pruning processes), and the disposal of MDF products are the main positive contributors, with similar magnitudes. For logging , the GHG emission comes from the residue decomposition, with 68% due to CO_2 and 26% due to CH_4. For the product disposal, since 45% of CLT is recycled to produce MDF at the end of life, the disposal of MDF plays a more critical role (MDF: 545 *vs* CLT: 139 t CO_2-eq emitted). The important contribution of MDF disposal to climate change is due to the CO_2 emitted during the incineration (mainly comes from the woody part).

Fig.7 Climate change impact for (a) BLc and (b) REFc. Processes with contributions lower than 1% of the total impact (in absolute) were attributed to categories others (+) or (-) (Process contributions were computed as follows: e.g., process A has a contribution of 1 and process B of -1, then the contribution of process A is 1/(abs(1)+abs(-1))=50%; details in SM). FU: functional unit.

For scenario REFc (Fig. 7b), natural grasslands and woody moorlands are shown as net contributors to the climate change impact. This reflects the emissions of CH_4 and N_2O due to the on-site decomposition of residues. Intensive grasslands and rapeseed lands contribute to the total negative score with 68% and 32% respectively, which in both cases is essentially due to

545 the avoided marginal vegetable oil (from rapeseed oil production) and marginal feed (from
546 rapeseed meal and silage production). Based on the results of section 3.2 (increase of 92040 kg
547 SOC ha^{-1} in 105 y), planting black locust increases, in average over the course of one rotation,
548 the CV-lands SOC by an amount equivalent to 112 t CO_2-eq, while maintaining the initial
549 vegetation leads to SOC decreases corresponding to 2 t CO_2–eq. Compared to the net results of
550 the two scenarios, the effect of the C change in soils is relatively small, representing 5% and 4%
551 of the net scores in scenario BLc and REFc, respectively.
552
553 **3.3.2 Other environmental impacts**
554 All impact results except climate change are presented in Fig. 8. Among all fifteen
555 environmental impacts of Fig. 8, there are four and twelve with a net positive score for scenario
556 BLc and REFc, respectively (Table 1, in red). Comparing scenario BLc to REFc, cultivating
557 black locust instead of the initial vegetation benefits all environmental impacts except ionizing
558 radiation, freshwater eutrophication, and land use.
559
560 Table 1. Summary of the impact results. Positive impact values on grey background. BLc is
561 better than REFc for the impacts highlited in italic bolds.

Impact	Unit	BLc	REFc
Climate change	kg CO2 eq	*-2202407*	-51061
Ozone depletion	kg CFC11 eq	*-0.034*	0.00488
Ionising radiation, HH	kBq U-235 eq	9937	1847
Photochemical ozone formation, HH	kg NMVOC eq	*-8217*	478
Respiratory inorganics	disease inc.	*-0.39*	0.030
Non-cancer human health effects	CTUh	*-0.17*	0.26
Cancer human health effects	CTUh	*-0.049*	0.0022
Acidification terrestrial and freshwater	mol H+ eq	*-4137*	4616
Eutrophication freshwater	kg P eq	407	-11.2
Eutrophication marine	kg N eq	*-1318*	883

Eutrophication terrestrial	mol N eq	*-13252*	21422
Ecotoxicity freshwater	CTUe	*-3767847*	-1002667
Land use	Pt	26884194	15617187
Water scarcity	m3 depriv.	*-8296011*	-460070
Resource use, energy carriers	MJ	*-45018209*	263511
Resource use, mineral and metals	kg Sb eq	*0.25*	1.49

Similar to climate change, avoided conventional products is the main contributor to the negative impact in scenario BLc. This particularly applies for plastic boards, especially due to the suspension polymerization operation (Fig. s6). However, the avoided use of plastic boards does not consistently translates with negative impacts. Without their incineration at the end-of-life, extra heat and electricity production are induced in the BLc system. Hence, avoiding the disposal of plastic boards generates burdens in ionizing radiation, freshwater eutrophication, and land use, representing 13%, 81%, and 46% of the positive scores, respectively. It also explained why in these three impacts, scenario BLc is worse than scenario REFc. In addition, in land use impact, rapeseed and silage ryegrass avoid palm oil and animal feed and the related necessary land, which reinforce this result.

In the scenario BLc, positive impact contributions come from multiple source across the different impacts, but agricultural management and products manufacturing tend to be two key contributors. The major agricultural management activities are tree logging processes (first- and second thinning, pruning, and harvesting). The diesel used in machines for logging and skidding trees to open-dry is the primary contributor, with some exceptions (e.g. PM_{10} from dust being the main contributor for respiratory inorganics). Since there is no fertilizer and pesticide use, the influence of black locust cultivation is negligible except in land use. Nevertheless, the agricultural activities during the cultivation (like the chemical application and diesel used for agricultural machines) are the main impact sources in scenario REFc, as observed in the LCA of common crops (Silva et al., 2014).

As widely admitted in woody board production (Piekarski et al., 2017; Yuan and Guo, 2017), the resin (urea-formaldehyde resin here) used as additive is the main positive score contributor (47%) in the manufacture chain, especially in mineral resource use. Furthermore, free formaldehyde emitted from the cure of urea-formaldehyde resin is another potential pitfall, causing more than half (56%) of positive score in cancer human health impact. Therefore, increasing the use of cellulosic materials in the fiberboard production for avoiding the resin use can be an efficient pathway to reduce the environmental impacts (Puettmann et al., 2016).

Fig. 8 LCA results for BLc (left bar) and REFc (right bar) scenarios for all impact categories of the EF method, with the exception of climate change.

3.4 Dynamic LCA results

3.4.1 Dynamic LCA in consequential modelling

GMTC results for the whole 269 years period considered (timeline in Fig. 4) are presented in Fig. 9. In the result analysis, distinction is made between the GHG (and related GMTC) stemming from the biomass (growth, decay, utilization, and end of life), noted as "bio", and the other GHGs coming from anthropogenic processes referenced as "non-bio" (despite stemming from biogenic processes like e.g., iLUC). The GMTC indicator has the property of additivity, thus the 'total' GMTC is the sum of GMTC from bio and non-bio contributors.

Concerning the REFc scenario, the GMTC (Total REFc; red curve) is positive during the cultivation period (up to 2126) except the first five years due to the avoided products. During the cultivation, 76% of captured CO_2 is released in a short time from the residue decomposition. Moreover, 3% of the C emited by anaerobic decoposition of residues is as CH_4, in the first ten years (2022-2031). The contribution of CH_4 represents up to 25% of REFc's bio GMTC, but this contribution decreases sharply (due to the short life time of CH_4 in athmosphere), shortly

after the last cultivation period, leading to the decrease of bio GMTC from 2131 onwards. Meanwhile, non-bio GMTC decreases continously because the main contributor is the avoided CO_2 from the replaced feedstock, a long-live GHG, thus with long term effect. The short lifespan of biogenic CH_4 and the relatively long-term CO_2 emissions from non-bio sources lead the non-bio GHG to dominate the trend of scenario REFc after the year 2150.

Fig. 9 GMTC results for all GHG sources from REFc and BLc scenarios, and the consequence of replacing REFc with BLc (Net GMTC). Total BLc = Bio BLc + Non bio BLc; Total REFc = Bio REFc + Non bio REFc; Net GMTC = Total BLc – Total REFc. 1st, 2nd, 3rd refer to the rotation number.

For the BLc scenario, in the first years of cultivation, the CO_2 captured is low and SOC mineralization is relatively high (Fig. 6b), making the bio GMTC slightly positive (Fig.9, Bio BLc). The BLc GMTC becomes negative in year 2028 (Fig. 9, Total BLc), reflecting, among others, the carbon captured in both biomass and as SOC as the black locust stand grows. The CH_4 contribution to bio GMTC represents a maximum of 9%, CO_2 being the largest contributor. The increase of bio GMTC (Bio BLc) after the last rotation is explained by the end of CO_2 capture, and the bio GHG emissions from the end of life incineration of MDF and CLT (the stored biogenic C is released back to the atmosphere).

The GMTC of non-bio sources (Non-bio BLc) is positive at the beginning, due to the emissions from tree plantation and iLUC. After the second thinning (year 2041), non-bio GMTC becomes negative, and between 2042 and 2047, closely follow the GMTC of bio BLc. However, from 2048 onwards, bio and non-bio GMTC drastically change paths, with non-bio GMTC importantly decreasing due to the plastic boards and bricks replacement by the bio-based products (MDF and CLT), involving manufacturing, use, and end-of-life processes. The

biggest GHG contributor is the avoided CO_2 emission from the plastic board life cycle. The avoided plastic boards are counted at the time when MDF is produced, namely during first and second thinning, harvesting, and CLT recycling (years 2032/2067/2102, 2042/2077/2112, 2057/2092/2127, 2108/2142/2178 respectively). The sharp decrease around 2057 is due to more plastic boards being avoided by more MDF being produced at the final harvest.

The net GMTC is negative just 5 years after the start of the first rotation, revealing that replacing the scenario REFc by BLc can mitigate global warming from the 5th year onwards. The mitigation effectiveness increases with the cultivation duration, with a peak around year 2136 (i.e. 10 years after the end of the last rotation), with a temperature reduction of -3.94E-09 K by ha of black locust cultivation. A minor part of the net negative GMTC is due to the bio flows, and reflect the higher CO_2 absorption of black locust compared to the initial vegetation. However, it is the non-bio GHG flows of BLc, and hence the avoided materials, that essentially determine the net GMTC result (Fig.9).

3.4.2 Dynamic LCA in attributional modeling

The GMTC results for the attributional perspective (average background processes with system expansion) are presented in Fig. 10, for REFa (top) and BLc (bottom) scenarios. The impact of each system is referenced as "net" REFa and BLc, obtained by the aggregation of all system's contributors. In this modeling approach, only the CO_2 capture processes result in negative GMTC, all other processes generate impacts, hence positive GMTC.

In REFa system, the bio REFa is the same as the bio REFc, and will accordingly not be further detailed. In the first decades, the impacts of agricultural management and later activities (Non-bio REFa), involving oil mill operation and ryegrass silage, are negligible compared to the GMTC from biogenic GHG flows. In REFa system, the biggest contributor is the plastic board (production, use, and end-of-life incineration), dominating the net REFa after 2043. CO_2

and CH_4, emitted as pulse in the years of MDF manufacture and disposal, are the primary contributors to GMTC, while conventional brick and heat production contribute little to the net GMTC result. The REFa system, despite its slightly negative net GMTC during the first years, is, as for REFc, shown as inadequate for global warming mitigation.

The net GMTC of the BLa system is negative in short and mid term with an overshot in the second halph of the century. Albeit very few studies exist combining carbon flows of the whole life cycle of the plant with dynamic GMTC evaluation, this kind of behavior with negative and positive domains was observed for other wood-based building materials (Negishi et al., 2019). The bio contributor of BLa scenario is the same as in consequential modeling and was analyzed in section 3.4.1. The non-bio GHG emissions stem from iLUC, wood logging operation, MDF&CLT production, disposal processes, and all related background processes, and always lead to positive GMTC. The GMTC from non-bio sources increases continuously, with sharp slopes when impulse emissions occur from these processes. At the end of anthropogenic activities, non-bio GMTC remains at a highe level for long term due to the accumulation of CO_2 (long lived gas) emitted during the whole time span. Because the CO_2 capture vanishes with the harvesting of wood, the net GMTC increases and becomes positive in 2072, then decreases sharply with the tree growth during the second rotation. Following the same trend, after the second rotation, the GMTC becomes positive for a while and continues to increase due to the non-bio contributors and additional processes. Concerning the additional products, induced feed ingredients affect the GMTC more than palm oil, CO_2 emission during the agricultural management being the major contributor.

Fig. 10. GMTC evolution in REFa (above) and BLa (bottom) scenario with time. 1st, 2nd, 3rd refer to the rotation number. Total BLa = Bio BLa + Non bio BLa; Net BLa = Total BLa+

Palm oil + Feed; Total VGa = Bio VGa + Non bio VGa; Net REFa = Total VGa + Heat + Plastic board + Brick.

3.5 Overall implications, limitations and perspectives

SOC enhancement was shown as a relatively minor contributor to climate change mitigation, given the important effect of avoided petrochemical plastic production and use. However, it should be highlighted that the SOC level simulated after three rotations (ca. 134000 kg ha^{-1}) is significantly higher than the average SOC in French lands covered by grass or forest (81000- 85000 kg ha^{-1}, Pellerin et al., 2021), and well above the 41000 kg ha^{-1} observed after 105 years of the initial vegetation system. Nevertheless, SOC deserves more attention and experimental investigation in real conditions in order to validate the simulation results. Such experiments will, in contrast to the simulation approach, require many years.

Combining the simulation results for the SOC, biomass growth, decay, and amount of products allows calculating the total C stock and comparing it to the C from CO_2 captured during the whole period (Fig. 11). The difference between stocks and captures represents the biogenic C released into the atmosphere (as CO_2 and CH_4). The C stock in products is higher than in soil. The net stock represents the negative emissions that the BL scenario could induce (81%, 39%, 15% of total captured C, in the year 2050, 2100, 2290 respectively. Fig. s11 in SM).

Annualizing the CO_2 absorption to compare with annual grass, black locust could capture twice the amount captured by the initial vegetation, similar to a vigorous energy grass (Hamelin et al., 2012). Compared to 14 wood species cultivated in France (Albers et al., 2019a), black locust could fix more C than the average of these species over the same period while attaining maturity well before the average maturity time of about 80 years.

Fig. 11 Carbon captured over the cultivation period, and biogenic carbon stocks during the lifetime of the BL scenario.

In the value chain proposed, bio-based products can replace fossil-based products with problematic environmental footprint at the level of their manufacturing and, significantly, of their end-of-life management.

The static LCA highlighted that replacing the initial vegetation with the black locust value chain is beneficial for the environment in 13 out of 16 environmental impacts (Table 1, italic fonts), mainly due to the fossil-based replacement. The use of resins/plastics in both bio-based and fossil-based products is critical in many impacts as highlighted by the LCA and confirmed by other studies (e.g., Nakano et al., 2018, Silva et al., 2013, etc.), therefore less or no resin additive is matter of investigation (Kouchaki-Penchah et al., 2016; Puettmann et al., 2016). The high environmental impacts of plastic production could be mitigated by other choices for the board material, as highlighted by the sensitivity analysis (SM section 5). Further, with the development of plastic recycling and replacement, less GHG emissions could be expected from production and incineration (Deng, 2014; Schwarz et al., 2021; Ye et al., 2017).

All conducted LCA modeling approaches indicate that the black locust system is generally better than the initial situation, either by measuring the consequence of this replacement as negative kg CO_2-eq and negative net GMTC, or by measuring/comparing the actual impact. BLa scenario could be a negative emission strategy in the near- and mid-term (2030-2063) when net GMTC is negative. It is certainly a mitigation solution from 2026- 2029, when the net GMTC is lower than that of REFa system but still positive (Fig. 10). The black locust system alone satisfies the neutrality in this decade (2027), but its implementation requires producing feedstock and oil elsewhere, hence attention must be paid to the net GMTC of the whole BLa system. Its increase in the second half of the century could be mitigated with

731 appropriate solutions at the level of all manufacturing and end-of-life technologies, i.e. less
732 fossil-based background processes and promoting wood material recycling instead of
733 incineration. If the systems are scaled-up to the whole CV-lands in France, the REFa system
734 increases the global mean temperature with 0.0020°C and 0.00576C by 2050 and 2100. BLa
735 system decreases the temperature with 0.0006°C in the mid-term, but increases it by 2100 with
736 0.0002°C, with a peak in between which must be mitigated. Of course, these values are only
737 orders of magnitude, to be relativized to the feasibility of using the whole CV-land potential.
738

739 **4 Conclusions**

740 This study investigated the relevance of using black locust as biopump to contribute to
741 global warming mitigation following the CSAAP concept. A value chain was proposed from
742 tree planting on CV-lands in France, to bio-based products manufacturing, use, and end of life,
743 as an alternative to leaving the CV-lands as they are presently. This system runs from the first
744 year of cultivation to the end of three rotations and to the end-of-life of the last product produced
745 from biomass, encompassing 267 years.

746 Simulation results of biomass growth, decay, and SOC changes showed, throughout
747 three rotations, that the black locust system induces more C stock in soils (considered as
748 negative emission) than the initial vegetation, for an annual average SOC increase of 21‰. This
749 also applies with regards to the C stored in the biomass of both systems. It was found that 15%
750 of the carbon captured by 3 rotations of black locust is still stocked in technosphere after 260
751 years.

752 Replacing the initial vegetation with the black locust value chain was shown to mitigate
753 global warming and was highlighted as beneficial to the environment for 13 of the 16 impact
754 categories evaluated through consequential LCA. Hence, improving climate change was shown
755 to result in minor trade-offs with the other environmental impacts. It should be noted that

avoided plastic, associated to the secondary product MDF, is key to climate change impact and to the performance of most other impacts.

Considering the climate goals, black locust value chain implementation results in climate cooling effect by net negative emissions, in the near and mid-term, but with a GMTC overshot (BLa) observed from the second half of the century, which must be mitigated. SOC has little contribution to carbon storage. Therefore, this study highlighted the importance of acting on emissions stemming from manufacturing and end-of-life (all background processes), which offset the benefit of C capture to achieve the goal of neutrality.

The dynamic approach used for global warming evaluation clearly shows that the mitigation potential is relative to the time scale. Approaching the end-of-life of the system results in emissions from land use change (if black locust is no more cultivated), and from the end-of-life management of the products, leading to the C stocks depletion and C emissions. Therefore, if such a strategy is implemented in reality, a continuous assessment of the carbon flows and other GHG is necessary, together with adapted solutions (e.g. recycling instead of landfilling, technologies with no emissions, etc.) to preserve the climate benefit.

Finally, these results highlight the benefit of using biopump for applying the CSAAP concept in mitigating climate change and other environmental impacts, providing the scientific basis for policy makers. However, there are some limitations that deserve further investigations. The carbon balance at the level of plant cultivation should be confirmed by experiments or specific investigation for each CV-land locally. In the practical applications, the land use cannot be guaranteed for such a long time, and the mono cultivation of one specie is unrealistic. Moreover, if all the available CV land in France were used for the planting of black locust and if all the wood were used only for the proposed products, the production would far exceed the market. Indeed, with the development of technology and market, there will be more and more

bio-based products instead of petrochemical materials, and the marginal products substituted in the consequential LCA will be challenged.

This study provided an integrated and comprehensive framework for proposing and analyzing mitigation solutions for global warming, which could be applied to other cases. Other combinations biopump/bio-based product could be analyzed; it is also possible to propose a panel of combined solutions with different plants and products for a given region.

Acknowledgments

This work was carried out within the research project Cambioscop (https://cambioscop.cnrs.fr), financed by the French National Research Agency, Programme Investissement d'Avenir (ANR-17-MGPA-0006) and Region Occitanie (18015981). Additional funding was supplied by the Chinese Scholarship Council (201801810082).

Supplementary material

Supplementary document contains : documented LCA inventory, details on modeling approaches, results.

References

Adamopoulos, S., Passialis, C., Voulgaridis, E., 2007. Strength properties of juvenile and mature wood in black locust (Robinia pseudoacacia L.). Wood Fiber Sci. 39, 241–249.

ADEME, 2018. Updated Energy-Climate Scenario ADEME 2035-2050.

Albers, A., Collet, P., Benoist, A., Hélias, A., 2019a. Data and non-linear models for the estimation of biomass growth and carbon fixation in managed forests. Data Br. 23. https://doi.org/10.1016/j.dib.2019.103841

Albers, A., Collet, P., Lorne, D., Benoist, A., Hélias, A., 2019b. Coupling partial-equilibrium and dynamic biogenic carbon models to assess future transport scenarios in France. Appl. Energy 239, 316–330. https://doi.org/10.1016/j.apenergy.2019.01.186

Andrade, C., Rangueil, A. De, Zamora-ledezma, E., Hamelin, L., 2022. A review on the interplay between bioeconomy and soil organic carbon stocks maintenance .

Barna, L.T., 2021. A climate goal – based , multicriteria method for system evaluation in life cycle assessment. Int. J. Life Cycle Assess. https://doi.org/10.1007/s11367-021-01991-1

Brandao, M., Martin, M., Cowie, A., Hamelin, L., Zamagni, A., 2017. Consequential Life Cycle Assessment: What, How, and Why? Encycl. Sustain. Technol. 1, 277–284. https://doi.org/10.1016/B978-0-12-409548-9.10068-5

Cadorel, X., Crawford, R., 2019. Life cycle analysis of cross laminated timber in buildings: a review. Engag. Archit. Sci. Meet. Challenges High. Density 52nd Int. Conf. Archit. Sci. Assoc. 2018 15978, 107–114.

Cardellini, G., Mutel, C.L., Vial, E., Muys, B., 2018. Temporalis, a generic method and tool for dynamic Life Cycle Assessment. Sci. Total Environ. 645, 585–595. https://doi.org/10.1016/j.scitotenv.2018.07.044

Chen, C.X., Pierobon, F., Ganguly, I., 2019. Life Cycle Assessment (LCA) of Cross-Laminated Timber (CLT) produced in Western Washington: The role of logistics and wood species mix. Sustain. 11. https://doi.org/10.3390/su11051278

Chen, D., Rojas, M., Samset, B.H., Cobb, K., Diongue-Niang, A., Edwards, P., Emori, S., Faria, S.H., Hawkins, E., Hope, P., Huybrechts, P., Meinshausen, M., Mustafa, S.K., Plattner, G.-K., Treguier, A.M., 2021. Framing, Context, and Methods., in: Climate Change 2021: The Physical Science Basis. Contribution of Working Group I to the Sixth Assessment Report of the Intergovernmental Panel on Climate Change. IPCC.

Chen, J., Zhang, H., Zhang, X., Tang, M., 2020. Arbuscular mycorrhizal symbiosis mitigates oxidative injury in black locust under salt stress through modulating antioxidant defence of the plant. Environ. Exp. Bot. 175, 104034. https://doi.org/10.1016/j.envexpbot.2020.104034

Ciccarese, L., Pellegrino, P., Silli, V., Zanchi, G., 2014. Short rotation forestry and methods for carbon accounting. A case study of black locust (Robinia pseudoacacia L.) plantation in central Italy. Rapporti 200, 5.

Clivot, H., Mouny, J.C., Duparque, A., Dinh, J.L., Denoroy, P., Houot, S., Vertès, F., Trochard, R., Bouthier, A., Sagot, S., Mary, B., 2019. Modeling soil organic carbon evolution in long-term arable experiments with AMG model. Environ. Model. Softw. 118, 99–113. https://doi.org/10.1016/j.envsoft.2019.04.004

Cordier, S., Blanchet, P., Robichaud, F., Amor, B., 2022. Dynamic LCA of the increased use of wood in buildings and its consequences: Integration of CO2 sequestration and material substitutions. Build. Environ. 226, 109695. https://doi.org/10.1016/j.buildenv.2022.109695

Corradini, G., Pierobon, F., Zanetti, M., 2019. Product environmental footprint of a cross-laminated timber system: a case study in Italy. Int. J. Life Cycle Assess. 24, 975–988. https://doi.org/10.1007/s11367-018-1541-x

Couret, L., Irle, M., Belloncle, C., Cathala, B., 2017. Extraction and characterization of cellulose nanocrystals from post-consumer wood fiberboard waste. Cellulose 24, 2125–2137. https://doi.org/10.1007/s10570-017-1252-7

Cowie, A.L., Berndes, G., Bentsen, N.S., Brandão, M., Cherubini, F., Egnell, G., George, B., Gustavsson, L., Hanewinkel, M., Harris, Z.M., Johnsson, F., Junginger, M., Kline, K.L., Koponen, K., Koppejan, J., Kraxner, F., Lamers, P., Majer, S., Marland, E., Nabuurs, G.J., Pelkmans, L., Sathre, R., Schaub, M., Smith, C.T., Soimakallio, S., Van Der Hilst,

F., Woods, J., Ximenes, F.A., 2021. Applying a science-based systems perspective to dispel misconceptions about climate effects of forest bioenergy. GCB Bioenergy 13, 1210–1231. https://doi.org/10.1111/gcbb.12844

da Costa, T.P., Quinteiro, P., Tarelho, L.A. da C., Arroja, L., Dias, A.C., 2018. Environmental impacts of forest biomass-to-energy conversion technologies: Grate furnace vs. fluidised bed furnace. J. Clean. Prod. 171, 153–162. https://doi.org/10.1016/j.jclepro.2017.09.287

Deng, Y., 2014. Life cycle assessment of biobased fibre-reinforced polymer composites. World Scientific. https://doi.org/10.1142/9789814566469_0063

Dodoo, A., Gustavsson, L., Sathre, R., 2014. Lifecycle primary energy analysis of low-energy timber building systems for multi-storey residential buildings. Energy Build. 81, 84–97. https://doi.org/10.1016/j.enbuild.2014.06.003

DRIAS CERFACS, IPSL, M.-F., 2013. CNRM-CERFACS-CM5/CNRM-ALADIN63-RCP4.5. DRIAS les Futur. du Clim.

ecoinvent, 2020. Ecoinvent 3.5 database [WWW Document]. URL https://www.ecoinvent.org/database/ecoinvent-37/new-data-in-ecoinvent-37/new-data-in-ecoinvent-37.html

European Commission-Joint Research Centre., 2010. General guide for life cycle assessment—detailed guidance. In: ILCD Handbook—International Reference Life Cycle Data System, first ed.

European Commission, 2021. EU Reference Scenario 2020 [WWW Document]. URL https://energy.ec.europa.eu/data-and-analysis/energy-modelling/eu-reference-scenario-2020_en

Fazio, S., Biganzioli, F., De Laurentiis, V., Zampori, L., Sala, S., Diaconu, E., 2018a. Supporting information to the characterisation factors of recommended EF Life Cycle Impact Assessment methods, version 2, from ILCD to EF 3.0, EUR 29600 EN, European

Commission, Ispra, 2018, ISBN 978-92-79-98584-3, doi:10.2760/002447, PUBSY No. JRC114822., New Models and Differences with ILCD, EUR. https://doi.org/10.2760/002447

Fazio, S., Zampori, L., A, D.S., Kusche, O., 2018b. Guide on Life Cycle Inventory (LCI) data generation for the Environmental Footprint. https://doi.org/10.2760/745658

Food and Agriculture Organization of the United Nations, 2020. GSOCmap v1.5.0 [WWW Document]. URL http://54.229.242.119/GSOCmap/

González-García, S., Gasol, C.M., Moreira, M.T., Gabarrell, X., Pons, J.R.I., Feijoo, G., 2011. Environmental assessment of black locust (Robinia pseudoacacia L.)-based ethanol as potential transport fuel. Int. J. Life Cycle Assess. 16, 465–477. https://doi.org/10.1007/s11367-011-0272-z

Göswein, V., Pittau, F., Silvestre, J.D., Freire, F., Habert, G., 2020. Dynamic life cycle assessment of straw-based renovation: A case study from a Portuguese neighbourhood. IOP Conf. Ser. Earth Environ. Sci. 588. https://doi.org/10.1088/1755-1315/588/4/042054

Guest, G., Cherubini, F., Strømman, A.H., 2013. Global Warming Potential of Carbon Dioxide Emissions from Biomass Stored in the Anthroposphere and Used for Bioenergy at End of Life. J. Ind. Ecol. 17, 20–30. https://doi.org/10.1111/j.1530-9290.2012.00507.x

Guo, H., Liu, Y., Meng, Y., Huang, H., Sun, C., Shao, Y., 2017. A Comparison of the energy saving and carbon reduction performance between reinforced concrete and cross-laminated timber structures in residential buildings in the severe cold region of China. Sustain. 9. https://doi.org/10.3390/su9081426

Hamelin, L., Jørgensen, U., Petersen, B.M., Olesen, J.E., Wenzel, H., 2012. Modelling the carbon and nitrogen balances of direct land use changes from energy crops in Denmark: A consequential life cycle inventory. GCB Bioenergy 4, 889–907. https://doi.org/10.1111/j.1757-1707.2012.01174.x

Hansen, J.H., Hamelin, L., Taghizadeh-Toosi, A., Olesen, J.E., Wenzel, H., 2020. Agricultural residues bioenergy potential that sustain soil carbon depends on energy conversion pathways. GCB Bioenergy 12, 1002–1013. https://doi.org/10.1111/gcbb.12733

IPCC, 2019. Refinement to the 2006 IPCC Guidelines for National Greenhouse Gas Inventories Volume 5 Waste, IPCC Good Practice Guidance and Uncertainty Management in National Greenhouse Gase Inventories.

ISO, 2006a. Environmental management: life cycle assessment; Principles and Framework. ISO.

ISO, 2006b. Environmental management: life cycle assessment; requirements and guidelines. ISO Geneva, Switzerland.

Jayalath, A., Navaratnam, S., Ngo, T., Mendis, P., Hewson, N., Aye, L., 2020. Life cycle performance of Cross Laminated Timber mid-rise residential buildings in Australia. Energy Build. 223, 110091. https://doi.org/10.1016/j.enbuild.2020.110091

Kassara, G., Pena Verrier, G., Chammas, M., Fournie, L., Mainsant, A., Marchal, D., Parrouffe, J.-M., 2019. Trajectories of evolution of the electricity mix 2020-2060: Additional analyses, FAQs, Report on data.

Keel, S.G., Leifeld, J., Mayer, J., Taghizadeh-Toosi, A., Olesen, J.E., 2017. Large uncertainty in soil carbon modelling related to method of calculation of plant carbon input in agricultural systems. Eur. J. Soil Sci. 68, 953–963. https://doi.org/10.1111/ejss.12454

Keresztesi, B., 1983. Breeding and cultivation of black locust, Robinia pseudoacacia, in Hungary. For. Ecol. Manage. 6, 217–244. https://doi.org/10.1016/S0378-1127(83)80004-8

Kouchaki-Penchah, H., Sharifi, M., Mousazadeh, H., Zarea-Hosseinabadi, H., 2016. Life cycle assessment of medium-density fiberboard manufacturing process in Islamic

Republic of Iran. J. Clean. Prod. 112, 351–358. https://doi.org/10.1016/j.jclepro.2015.07.049

Lan, K., Kelley, S.S., Nepal, P., Yao, Y., 2020. Dynamic life cycle carbon and energy analysis for cross-laminated timber in the Southeastern United States. Environ. Res. Lett. 15, 124036. https://doi.org/10.1088/1748-9326/abc5e6

Launay, C., Constantin, J., Chlebowski, F., Houot, S., Graux, A.I., Klumpp, K., Martin, R., Mary, B., Pellerin, S., Therond, O., 2021. Estimating the carbon storage potential and greenhouse gas emissions of French arable cropland using high-resolution modeling. Glob. Chang. Biol. 27, 1645–1661. https://doi.org/10.1111/gcb.15512

Minasny, B., Malone, B.P., McBratney, A.B., Angers, D.A., Arrouays, D., Chambers, A., Chaplot, V., Chen, Z.S., Cheng, K., Das, B.S., Field, D.J., Gimona, A., Hedley, C.B., Hong, S.Y., Mandal, B., Marchant, B.P., Martin, M., McConkey, B.G., Mulder, V.L., O'Rourke, S., Richer-de-Forges, A.C., Odeh, I., Padarian, J., Paustian, K., Pan, G., Poggio, L., Savin, I., Stolbovoy, V., Stockmann, U., Sulaeman, Y., Tsui, C.C., Vågen, T.G., van Wesemael, B., Winowiecki, L., 2017. Soil carbon 4 per mille. Geoderma 292, 59–86. https://doi.org/10.1016/j.geoderma.2017.01.002

Nakano, K., Ando, K., Takigawa, M., Hattori, N., 2018. Life cycle assessment of wood-based boards produced in Japan and impact of formaldehyde emissions during the use stage. Int. J. Life Cycle Assess. 23, 957–969. https://doi.org/10.1007/s11367-017-1343-6

Negishi, K., Lebert, A., Almeida D., Chevalier J., Tiruta-Barna, L., 2019, Evaluating climate change pathways through a building's lifecycle based on Dynamic Life Cycle Assessment, Building and Environment, 164, 2019, 106377

Nicolescu, V.N., Hernea, C., Bakti, B., Keserű, Z., Antal, B., Rédei, K., 2018. Black locust (Robinia pseudoacacia L.) as a multi-purpose tree species in Hungary and Romania: a review. J. For. Res. 29, 1449–1463. https://doi.org/10.1007/s11676-018-0626-5

Nicolescu, V.N., Rédei, K., Mason, W.L., Vor, T., Pöetzelsberger, E., Bastien, J.C., Brus, R., Benčať, T., Đodan, M., Cvjetkovic, B., Andrašev, S., La Porta, N., Lavnyy, V., Mandžukovski, D., Petkova, K., Roženbergar, D., Wąsik, R., Mohren, G.M.J., Monteverdi, M.C., Musch, B., Klisz, M., Perić, S., Keça, L., Bartlett, D., Hernea, C., Pástor, M., 2020. Ecology, growth and management of black locust (Robinia pseudoacacia L.), a non-native species integrated into European forests. J. For. Res. 31, 1081–1101. https://doi.org/10.1007/s11676-020-01116-8

Onyeaju, M.C., Osarolube, E., Chukwuocha, E.O., Ekuma, C.E., Omasheye, G.A.J., 2012. Comparison of the Thermal Properties of Asbestos and Polyvinylchloride (PVC) Ceiling Sheets. Mater. Sci. Appl. 03, 240–244. https://doi.org/10.4236/msa.2012.34035

Pehme, S., Veromann, E., Hamelin, L., 2017. Environmental performance of manure co-digestion with natural and cultivated grass – A consequential life cycle assessment. J. Clean. Prod. 162, 1135–1143. https://doi.org/10.1016/j.jclepro.2017.06.067

Pellerin, S., Bamière, L., Savini, I., Réchauchère, O., 2021. Stocker du carbone dans les sols français. Quel potentiel au regard de l'objectif 4 pour 1000 et à quel coût? Stock. du carbone dans les sols français. https://doi.org/10.35690/978-2-7592-3149-2

Petersen, B.M., Berntsen, J., Hansen, S., Jensen, L.S., 2005. CN-SIM - A model for the turnover of soil organic matter. I. Long-term carbon and radiocarbon development. Soil Biol. Biochem. 37, 359–374. https://doi.org/10.1016/j.soilbio.2004.08.006

Petersen, B.M., Knudsen, M.T., Hermansen, J.E., Halberg, N., 2013. An approach to include soil carbon changes in life cycle assessments. J. Clean. Prod. 52, 217–224. https://doi.org/10.1016/j.jclepro.2013.03.007

Piekarski, C.M., de Francisco, A.C., da Luz, L.M., Kovaleski, J.L., Silva, D.A.L., 2017. Life cycle assessment of medium-density fiberboard (MDF) manufacturing process in Brazil. Sci. Total Environ. 575, 103–111. https://doi.org/10.1016/j.scitotenv.2016.10.007

Puettmann, M., Bergman, R., Oneil, E., 2016. Cradle to gate life cycle assessment of north American cellulosic fiberboard production. CORRIM Final Report. Univ. Washington. Seattle, WA. January 2016. 66 p. 1–66.

Rédei, K., Csiha, I., KeserU, Z., Gál, J., 2012. Influence of regeneration method on the yield and stem quality of black locust (Robinia pseudoacacia L.) Stands: A case study. Acta Silv. Lignaria Hungarica 8, 103–112. https://doi.org/10.2478/v10303-012-0008-1

Rédei, K., Csiha, I., Keseru, Z., Rásó, J., Kamandiné Végh, Á., Antal, B., 2014. Growth and Yield of Black Locust (Robinia pseudoacacia L.) Stands in Nyírség Growing Region (North-East Hungary). South-east Eur. For. 5, 13–22. https://doi.org/10.15177/seefor.14-04

Saez de Bikuña, K., Hamelin, L., Hauschild, M.Z., Pilegaard, K., Ibrom, A., 2018. A comparison of land use change accounting methods: seeking common grounds for key modeling choices in biofuel assessments. J. Clean. Prod. 177, 52–61. https://doi.org/10.1016/j.jclepro.2017.12.180

Sahoo, K., Bergman, R., Alanya-Rosenbaum, S., Gu, H., Liang, S., 2019. Life cycle assessment of forest-based products: A review. Sustain. 11, 1–30. https://doi.org/10.3390/su11174722

Schaubroeck, T., Schaubroeck, S., Heijungs, R., Zamagni, A., Brandão, M., Benetto, E., 2021. Attributional & consequential life cycle assessment: Definitions, conceptual characteristics and modelling restrictions. Sustain. 13. https://doi.org/10.3390/su13137386

Schwarz, A.E., Ligthart, T.N., Godoi Bizarro, D., De Wild, P., Vreugdenhil, B., van Harmelen, T., 2021. Plastic recycling in a circular economy; determining environmental performance through an LCA matrix model approach. Waste Manag. 121, 331–342. https://doi.org/10.1016/j.wasman.2020.12.020

Seserman, D.M., Pohle, I., Veste, M., Freese, D., 2018. Simulating climate change impacts on hybrid-poplar and black locust short rotation coppices. Forests 9, 1–25. https://doi.org/10.3390/f9070419

Shen, Z., Tiruta-Barna, L., Hamelin, L., 2022a. From Hemp Grown on Carbon Vulnerable Lands to Long-Lasting Bio-Based Products: Uncovering Trade-Offs between Overall Environmental Impacts, Sequestration in Soils and Dynamic Influence on Global Temperature. Sequestration Soils Dyn. Influ. Glob. Temp.

Shen, Z., Tiruta-Barna, L., Karan S. K., Hamelin, L., 2022b, Simultaneous carbon storage in arable land and anthropogenic products (CSAAP): Demonstrating an integrated concept towards well below 2◦C. Resour. Conserv. Recycl. 182, 106293. https://doi.org/10.1016/j.resconrec.2022.106293

Silva, D.A.L., Lahr, F.A.R., Garcia, R.P., Freire, F.M.C.S., Ometto, A.R., 2013. Life cycle assessment of medium density particleboard (MDP) produced in Brazil. Int. J. Life Cycle Assess. 18, 1404–1411. https://doi.org/10.1007/s11367-013-0583-3

Silva, D.A.L., Lahr, F.A.R., Pavan, A.L.R., Saavedra, Y.M.B., Mendes, N.C., Sousa, S.R., Sanches, R., Ometto, A.R., 2014. Do wood-based panels made with agro-industrial residues provide environmentally benign alternatives? An LCA case study of sugarcane bagasse addition to particle board manufacturing. Int. J. Life Cycle Assess. 19, 1767–1778. https://doi.org/10.1007/s11367-014-0776-4

Stocker, T.F., Qin, D., Plattner, G.K., Tignor, M.M.B., Allen, S.K., Boschung, J., Nauels, A., Xia, Y., Bex, V., Midgley, P.M., 2013. Climate change 2013 the physical science basis: Working Group I contribution to the fifth assessment report of the intergovernmental panel on climate change. Clim. Chang. 2013 Phys. Sci. Basis Work. Gr. I Contrib. to Fifth Assess. Rep. Intergov. Panel Clim. Chang. 9781107057, 1–1535. https://doi.org/10.1017/CBO9781107415324

Stone, K.R., 2009. Robinia pseudoacacia. In: Fire Effects Information System [WWW Document]. U.S. Dep. Agric. For. Serv. Rocky Mt. Res. Station. Fire Sci. Lab. URL https://www.fs.fed.us/database/feis/plants/tree/robpse/all.html

Taghizadeh-Toosi, A., Glendining, M., Vejlin, J., Hutchings, N.J., Olesen, J.E., Christensen, B.T., Kätterer, T., 2014. C-TOOL: A simple model for simulating whole-profile carbon storage in temperate agricultural soils. Ecol. Modell. 292, 11–25. https://doi.org/10.1016/j.ecolmodel.2014.08.016

Takano, A., Hughes, M., Winter, S., 2014. A multidisciplinary approach to sustainable building material selection: A case study in a Finnish context. Build. Environ. 82, 526–535. https://doi.org/10.1016/j.buildenv.2014.09.026

Tonini, D., Hamelin, L., Astrup, T.F., 2016. Environmental implications of the use of agro-industrial residues for biorefineries: application of a deterministic model for indirect land-use changes. GCB Bioenergy 8, 690–706. https://doi.org/10.1111/gcbb.12290

Wang, B., Liu, G., Xue, S., 2012. Effect of black locust (Robinia pseudoacacia) on soil chemical and microbiological properties in the eroded hilly area of China's loess plateau. Environ. Earth Sci. 65, 597–607. https://doi.org/10.1007/s12665-011-1107-8

Wang, J.J., Hu, C.X., Bai, J., Gong, C.M., 2015. Carbon sequestration of mature black locust standson the loess plateau, China. Plant, Soil Environ. 61, 116–121. https://doi.org/10.17221/931/2014-PSE

Warne, A., 2016. Black locust (Robinia pseudoacacia L.). Best management practices in Ontario, Ontario invasive plant council, Peterborough.

Yang, Y., Tilman, D., 2020. Soil and root carbon storage is key to climate benefits of bioenergy crops. Biofuel Res. J. 7, 1143–1148. https://doi.org/10.18331/BRJ2020.7.2.2

Ye, L., Qi, C., Hong, J., Ma, X., 2017. Life cycle assessment of polyvinyl chloride production and its recyclability in China. J. Clean. Prod. 142, 2965–2972. https://doi.org/10.1016/j.jclepro.2016.10.171

Yuan, Y., Guo, M., 2017. Do green wooden composites using lignin-based binder have environmentally benign alternatives? A preliminary LCA case study in China. Int. J. Life Cycle Assess. 22, 1318–1326. https://doi.org/10.1007/s11367-016-1235-1

Żelazna, A., Kraszkiewicz, A., Przywara, A., Łagód, G., Suchorab, Z., Werle, S., Ballester, J., Nosek, R., 2019. Life cycle assessment of production of black locust logs and straw pellets for energy purposes. Environ. Prog. Sustain. Energy 38, 163–170. https://doi.org/10.1002/ep.13043

Zieger, V., Lecompte, T., Hellouin de Menibus, A., 2020. Impact of GHGs temporal dynamics on the GWP assessment of building materials: A case study on bio-based and non-bio-based walls. Build. Environ. 185, 107210. https://doi.org/10.1016/j.buildenv.2020.107210

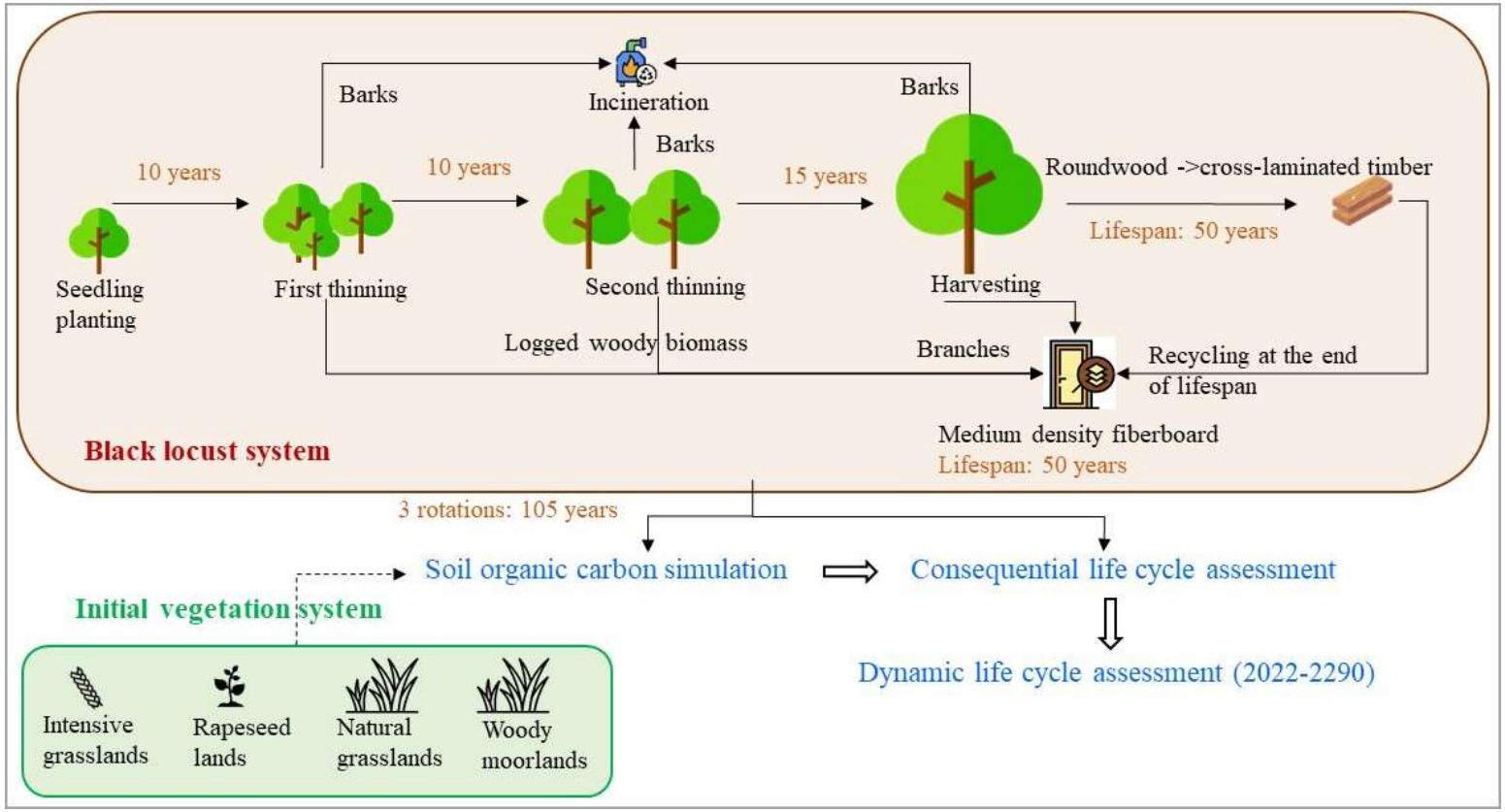

Graphical Abstract

(a) Black locust- cultivation, harvesting and pretreatment

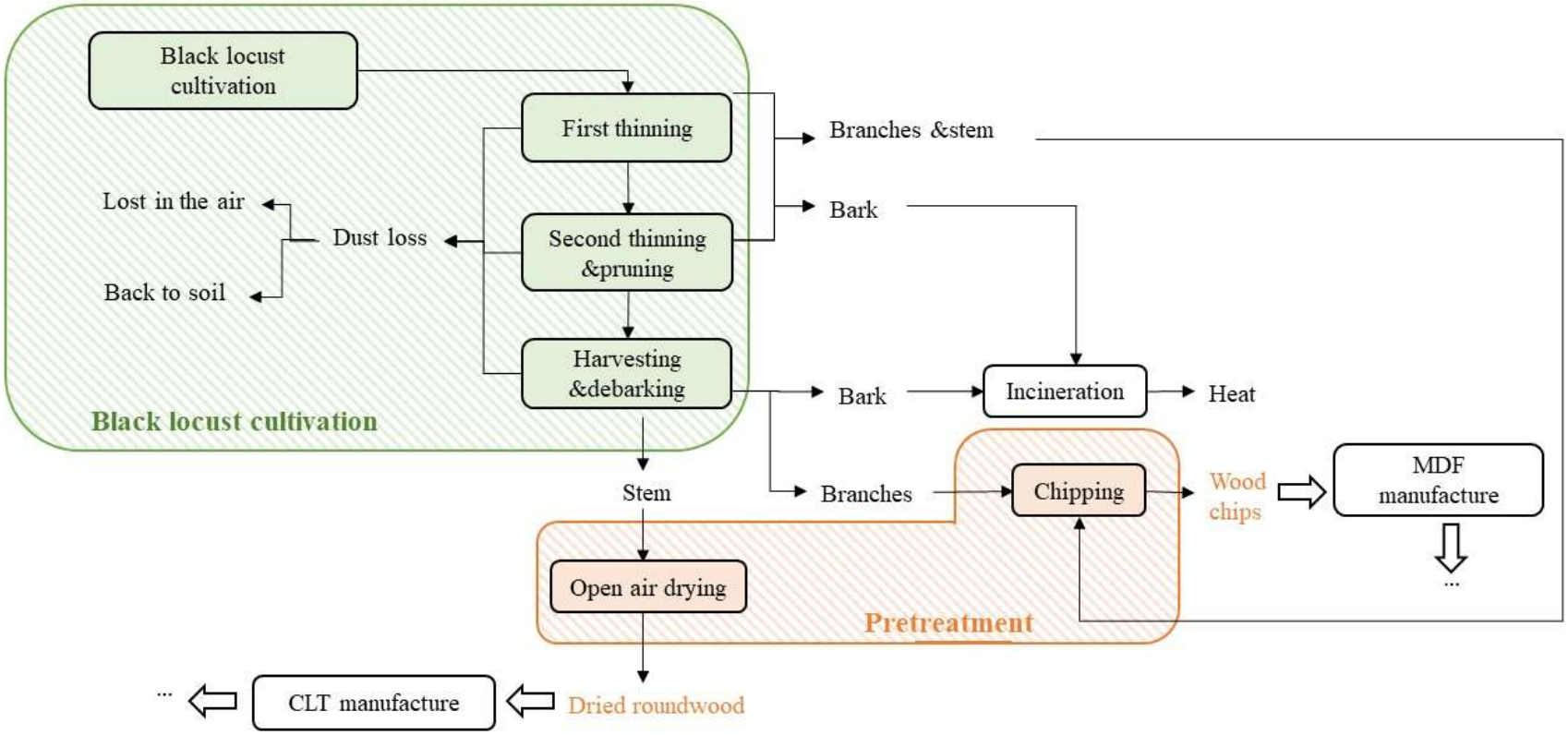

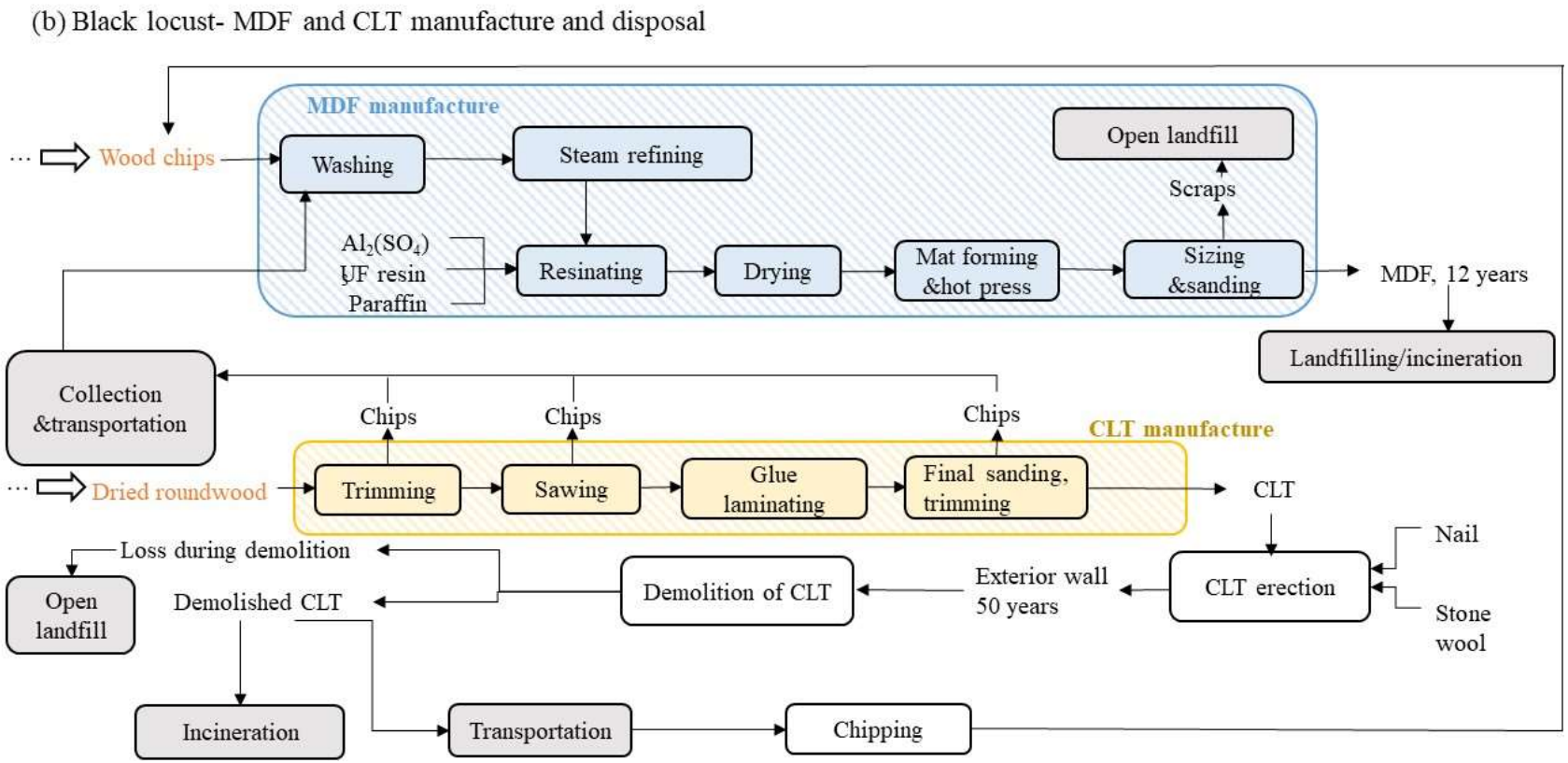

Fig. 1 Process flow diagram showing the key activities considered for (a) black locust cultivation, harvesting (green) and residual biomass management (orange), and (b) manufacture and disposal of cross-laminated timber (CLT; yellow) and medium density fiberboard (MDF; blue

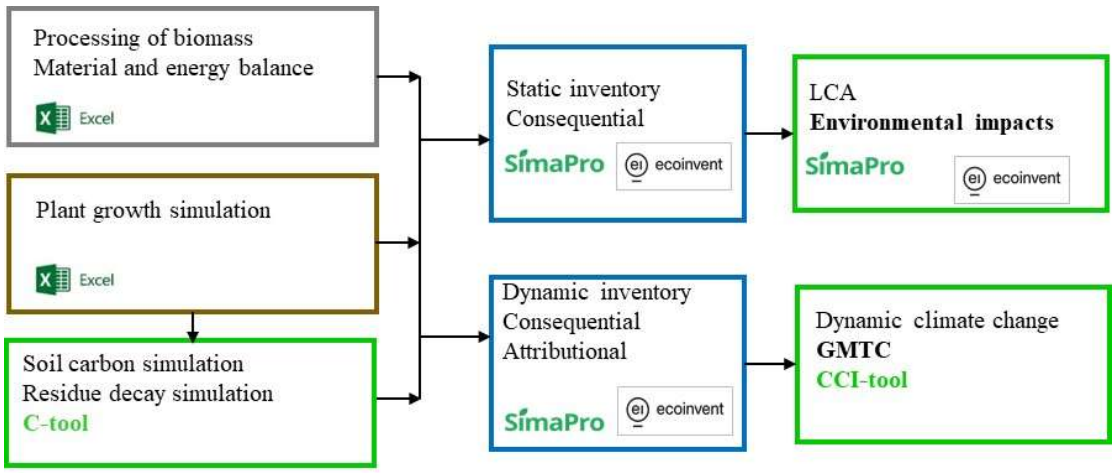

Fig. 2 Calculation steps followed in this study

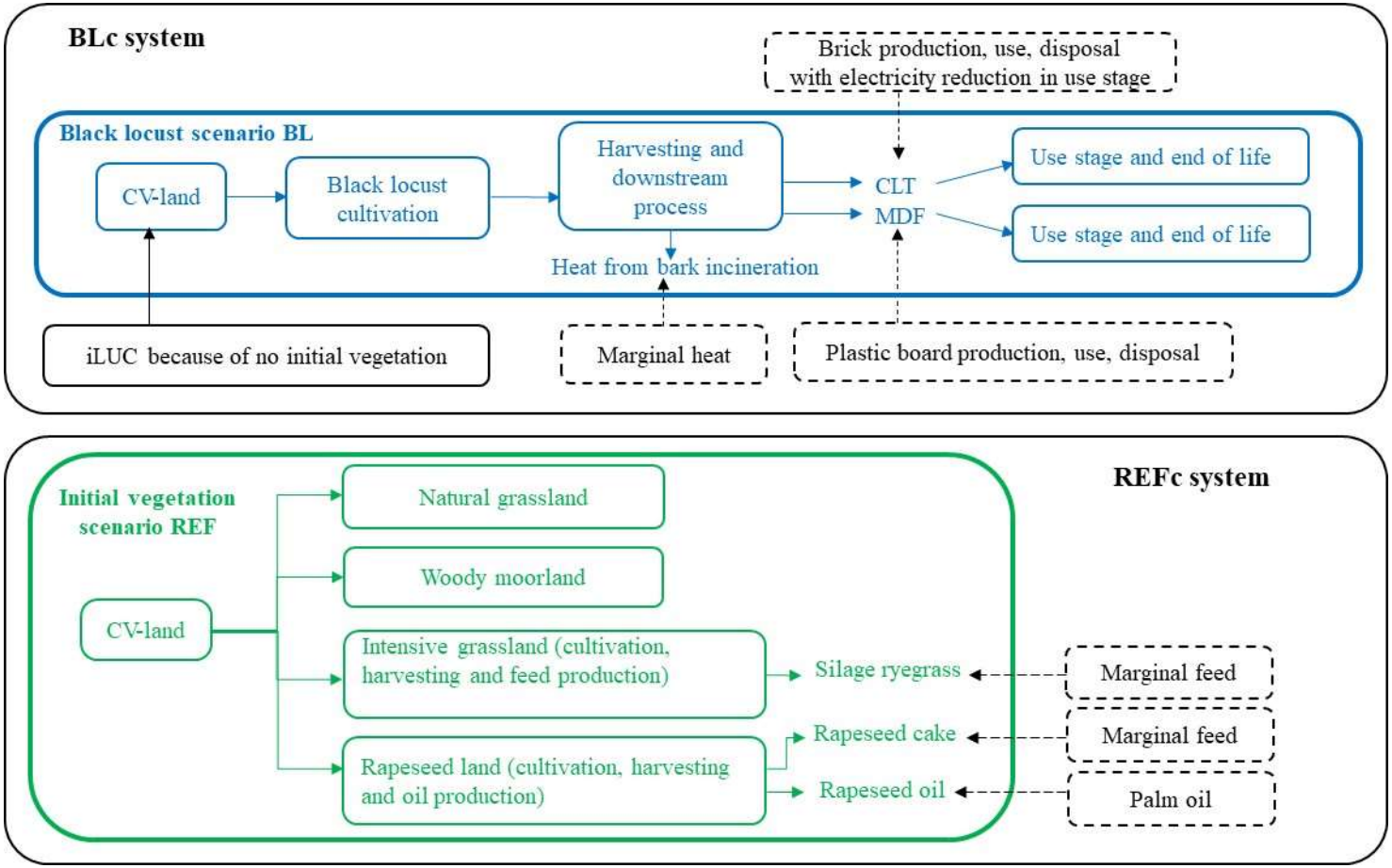

Fig. 3 System diagrams showing the boundaries considered in consequential LCA of business as usual (REFc) and black locust (BLc) systems, built on REF and BL scenarios respectively. CV-land: carbon vulnerable land; iLUC: Indirect land use changes; CLT: cross-laminated timber; MDF: medium density fiberboard. Full lines indicate induced processes while dotted lines represent avoided processes.

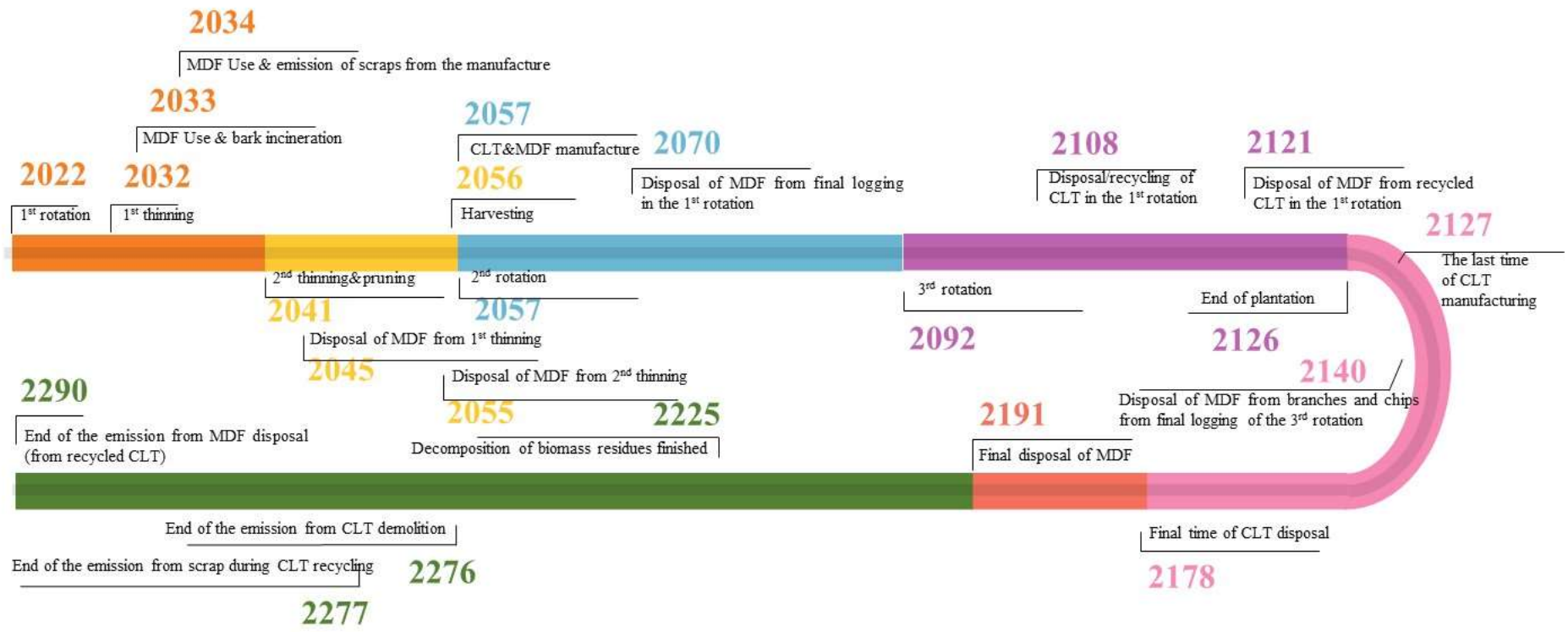

Fig. 4 Timeline of processes for dynamic LCA.

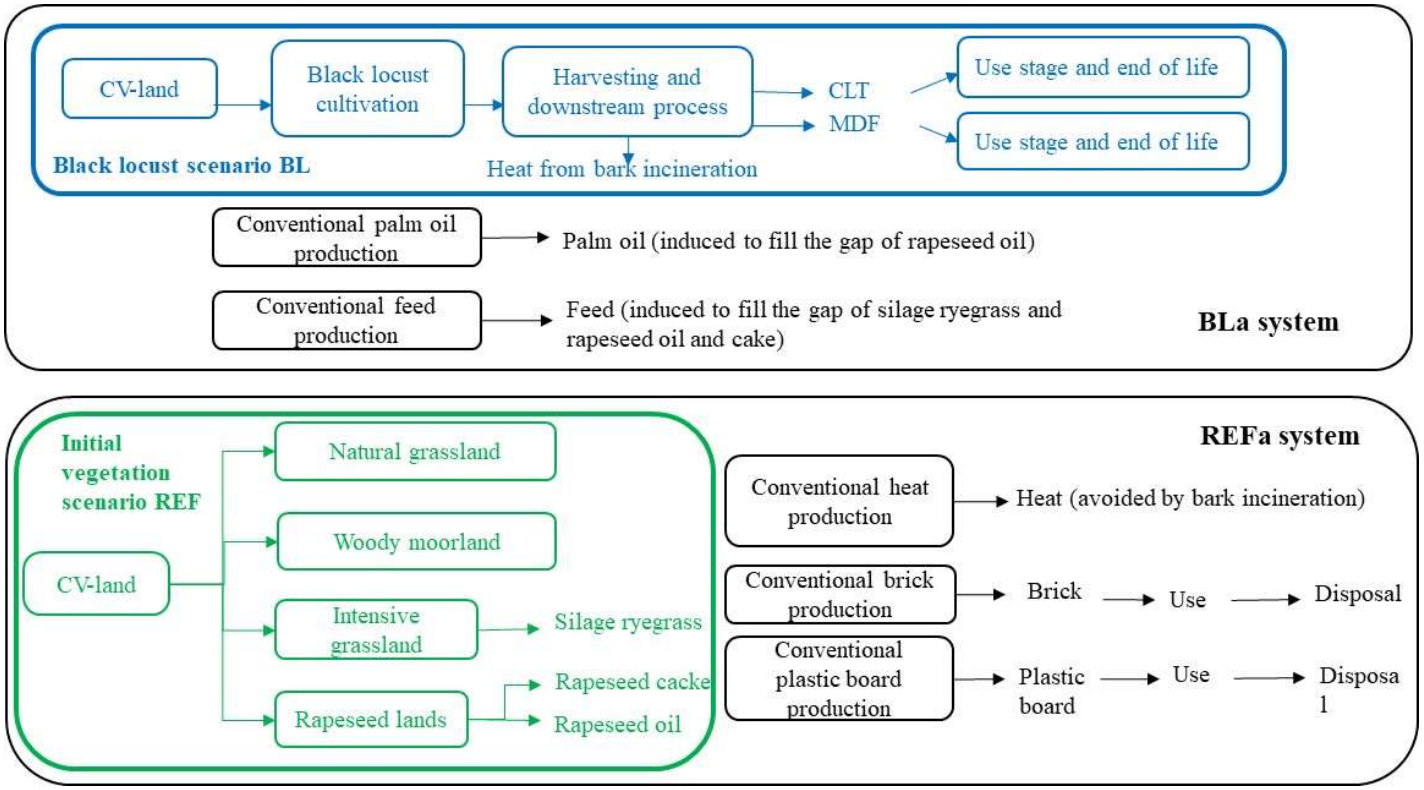

Fig. 5 System diagrams of business as usual (REFa) and black locust (BLa) systems, built on REF and BL scenarios respectively.

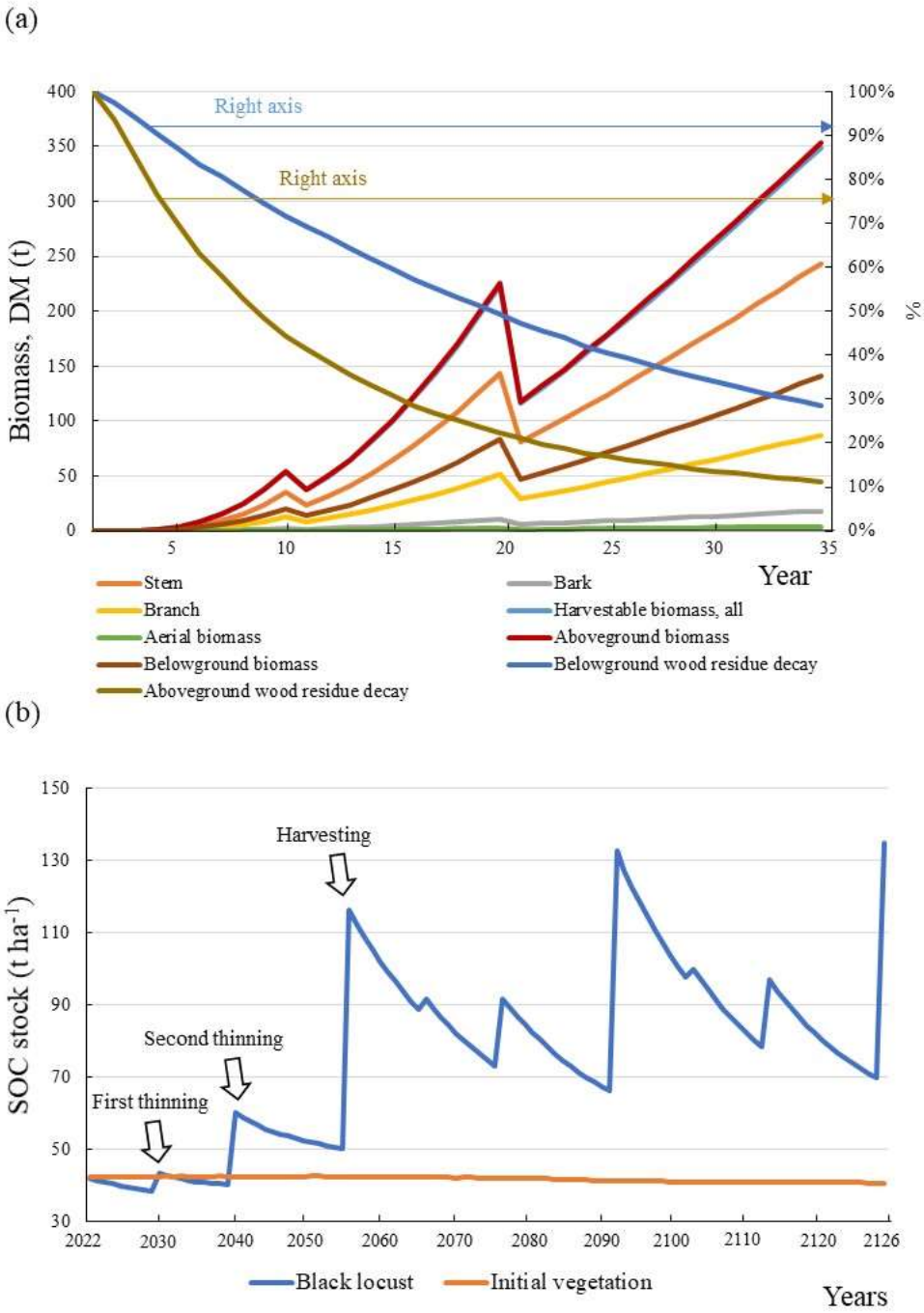

Fig. 6 Simulated (a) biomass growth and decay for black locust during one rotation, and (b) SOC evolution for black locust and initial vegetation during the cultivation period. Harvestable biomass: stem, branch and bark.

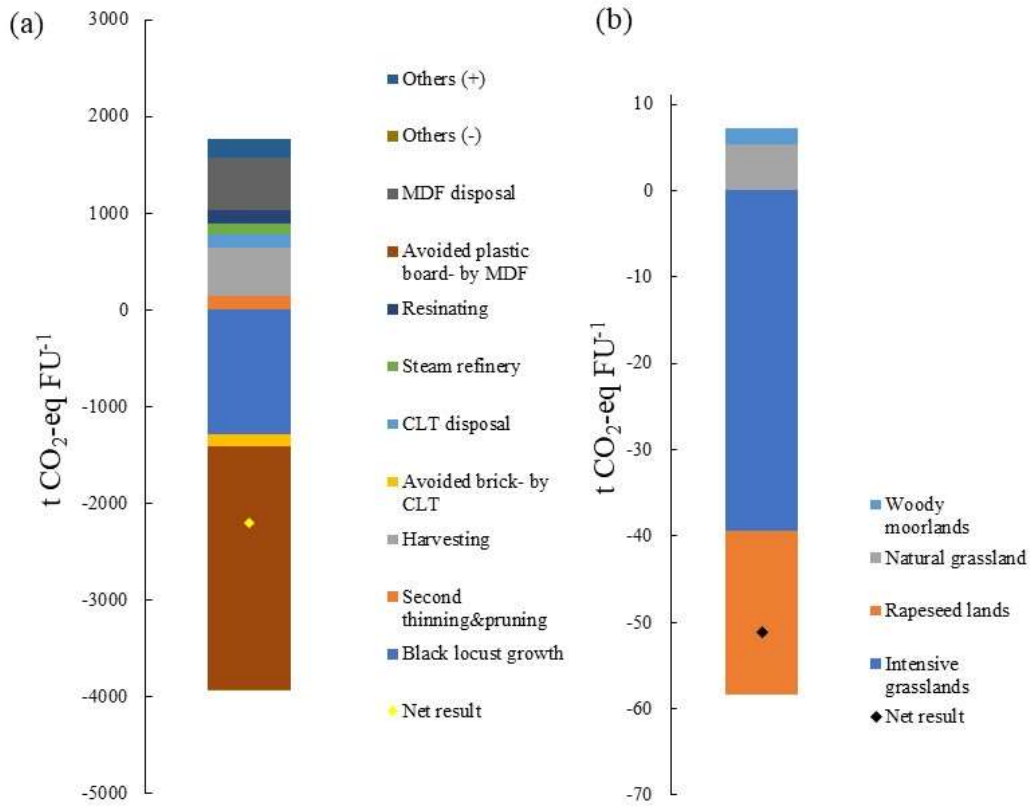

Fig.7 Climate change impact for (a) BLc and (b) REFc. Processes with contributions lower than 1% of the total impact (in absolute) were attributed to categories others (+) or (-) (Process contributions were computed as follows: e.g., process A has a contribution of 1 and process B of -1, then the contribution of process A is 1/(abs(1)+abs(-1))=50%; details in SM). FU: functional unit.

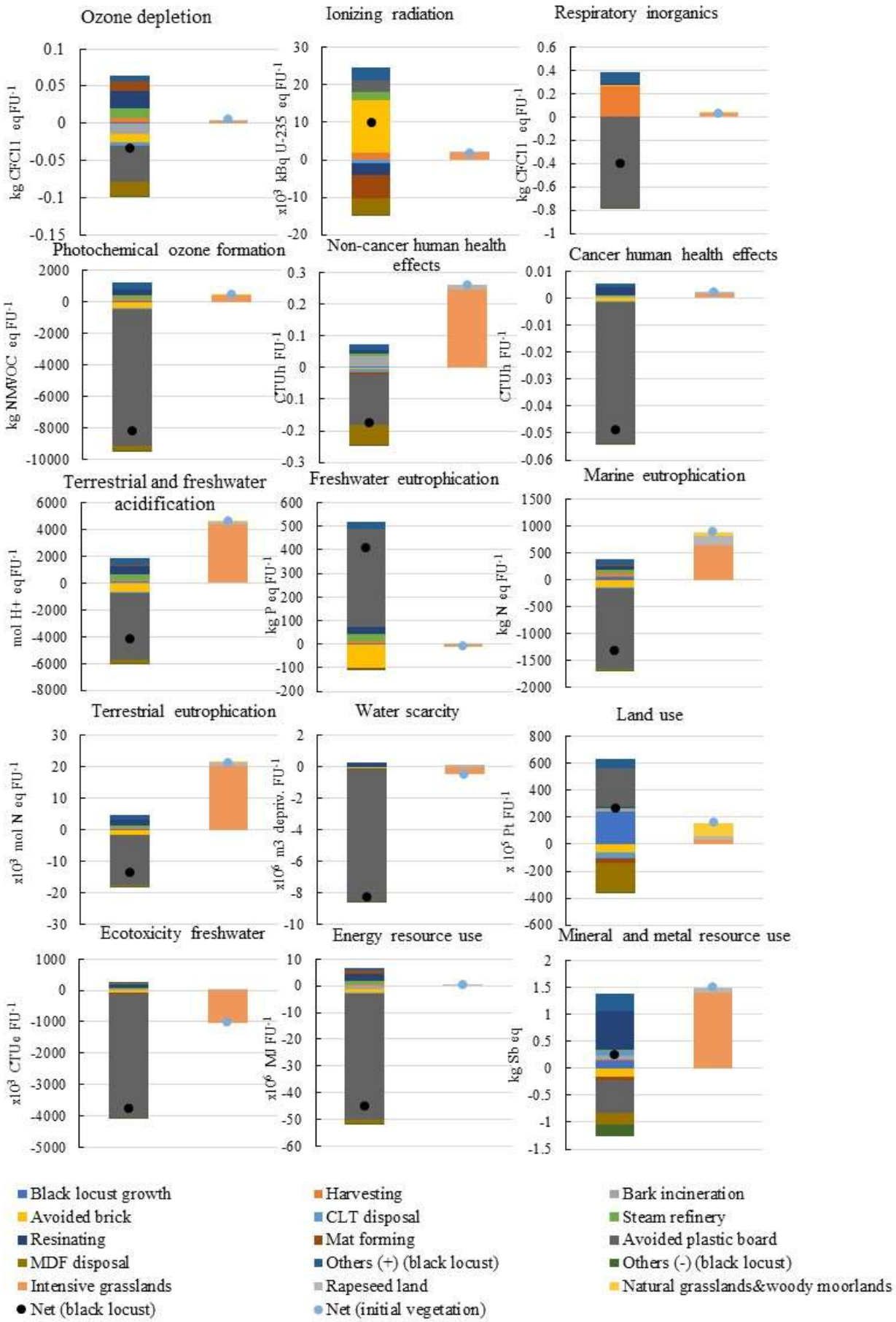
Ozone depletion
kg CFCl1 eq FU-1
Ionizing radiation
x10³ kBq U-235 eq FU-1
Respiratory inorganics
kg CFCl1 eq FU-1
Photochemical ozone formation
kg NMVOC eq FU-1
Non-cancer human health effects
CTUh FU-1
Cancer human health effects
CTUh FU-1
Terrestrial and freshwater acidification
mol H+ eq FU-1
Freshwater eutrophication
kg P eq FU-1
Marine eutrophication
kg N eq FU-1
Terrestrial eutrophication
x10³ mol N eq FU-1
Water scarcity
x10⁶ m3 depriv. FU-1
Land use
x 10⁵ Pt FU-1
Ecotoxicity freshwater
x10³ CTUe FU-1
Energy resource use
x10⁶ MJ FU-1
Mineral and metal resource use
kg Sb eq
Black locust growth
Harvesting
Bark incineration
Avoided brick
CLT disposal
Steam refinery
Resinating
Mat forming
Avoided plastic board
MDF disposal
Others (+) (black locust)
Others (-) (black locust)
Intensive grasslands
Rapeseed land
Natural grasslands&woody moorlands
Net (black locust)
Net (initial vegetation)

Fig. 8 LCA results for BLc (left bar) and REFc (right bar) scenarios for all impact categories of the EF method, with the exception of climate change impact.

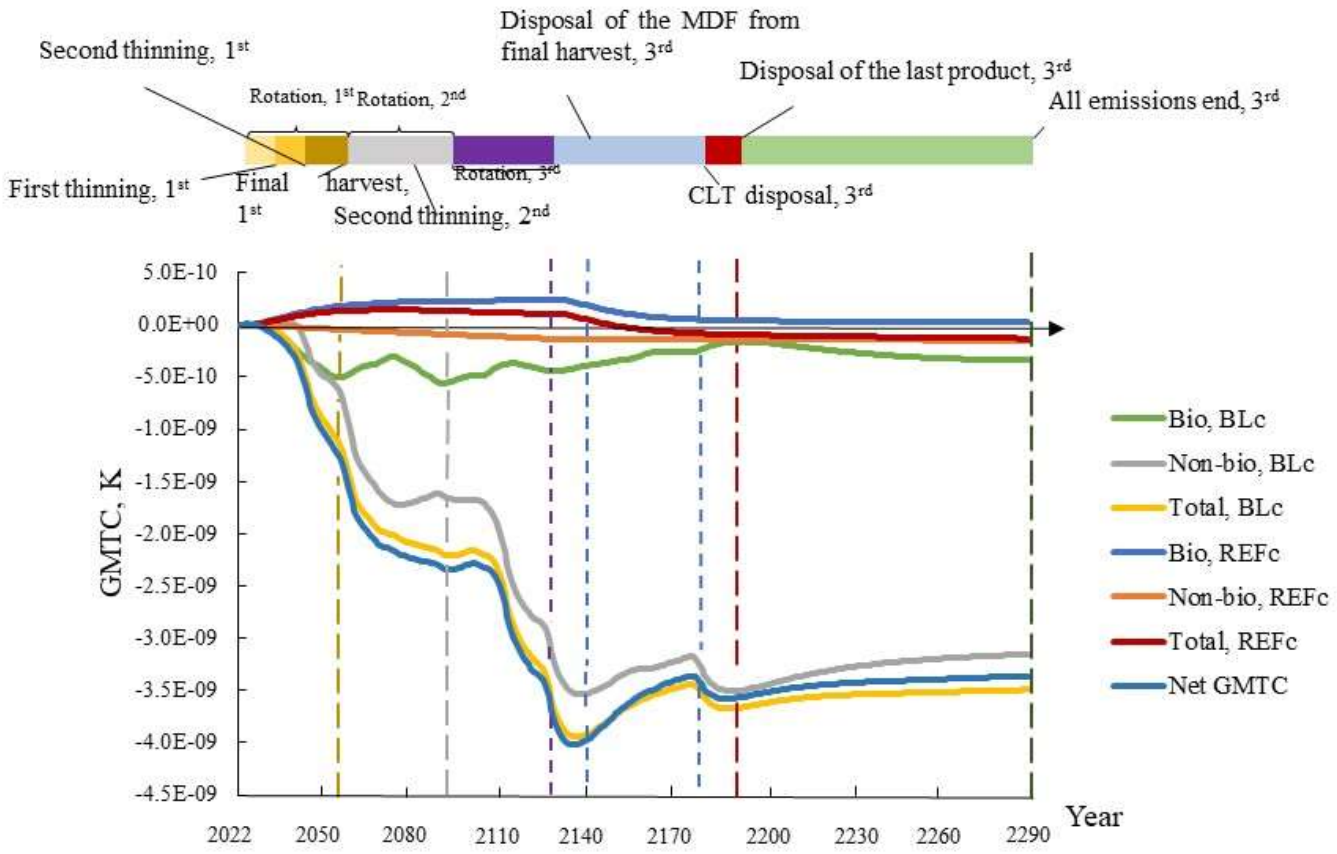

Fig. 9 GMTC results for all GHG sources from REFc and BLc scenarios, and the consequence of replacing REFc with BLc (Net GMTC). Total BLc = Bio BLc + Non bio BLc; Total REFc = Bio REFc + Non bio REFc; Net GMTC = Total BLc – Total REFc. 1st, 2nd, 3rd refer to the rotation number.

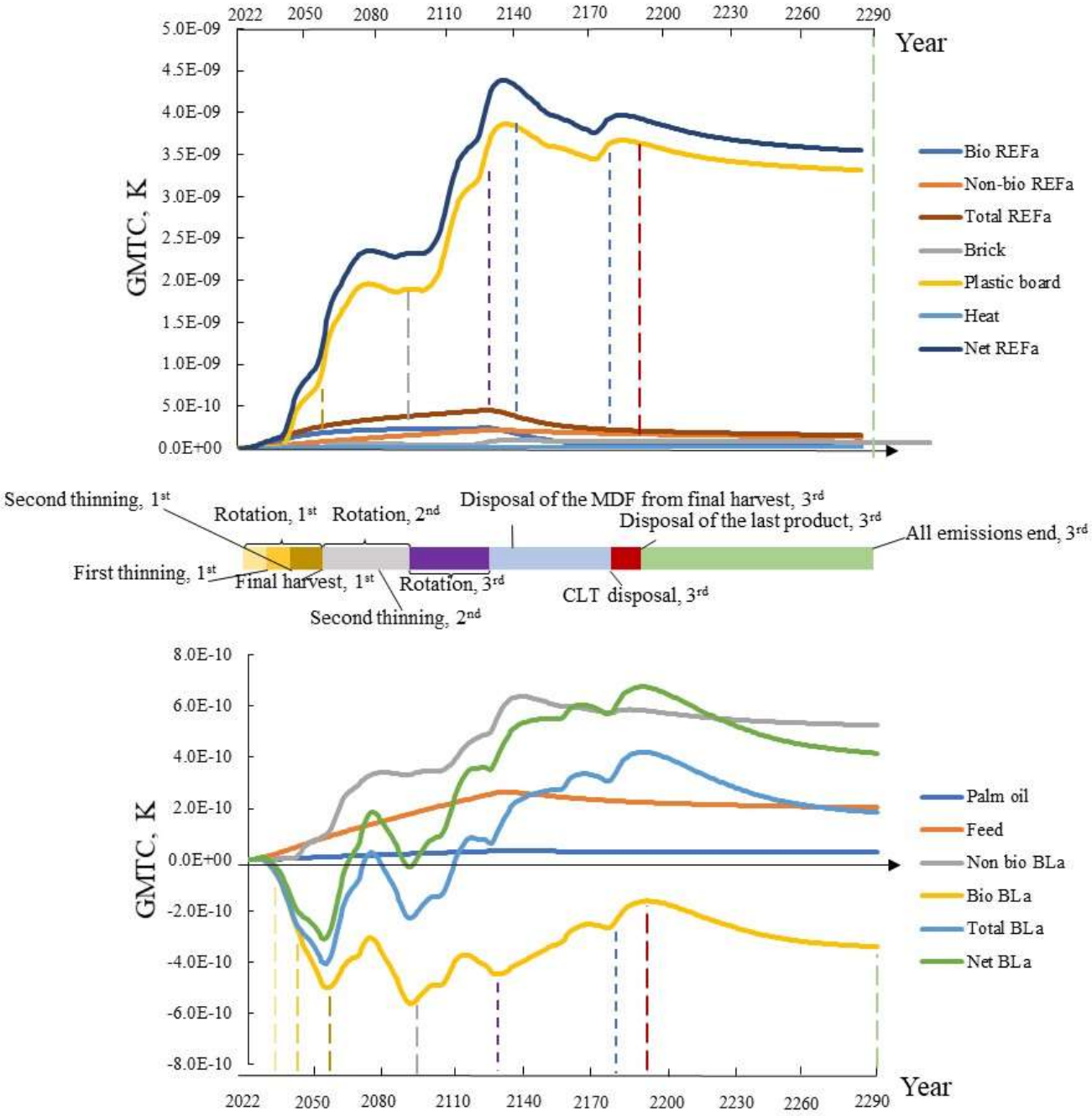

Fig. 10. GMTC evolution in REFa (above) and BLa (bottom) scenario with time. 1st, 2nd, 3rd refer to the rotation number. Total BLa = Bio BLa + Non bio BLa; Net BLa = Total BLa+ Palm oil + Feed; Total VGa = Bio VGa + Non bio VGa; Net REFa = Total VGa + Heat + Plastic board + Brick.

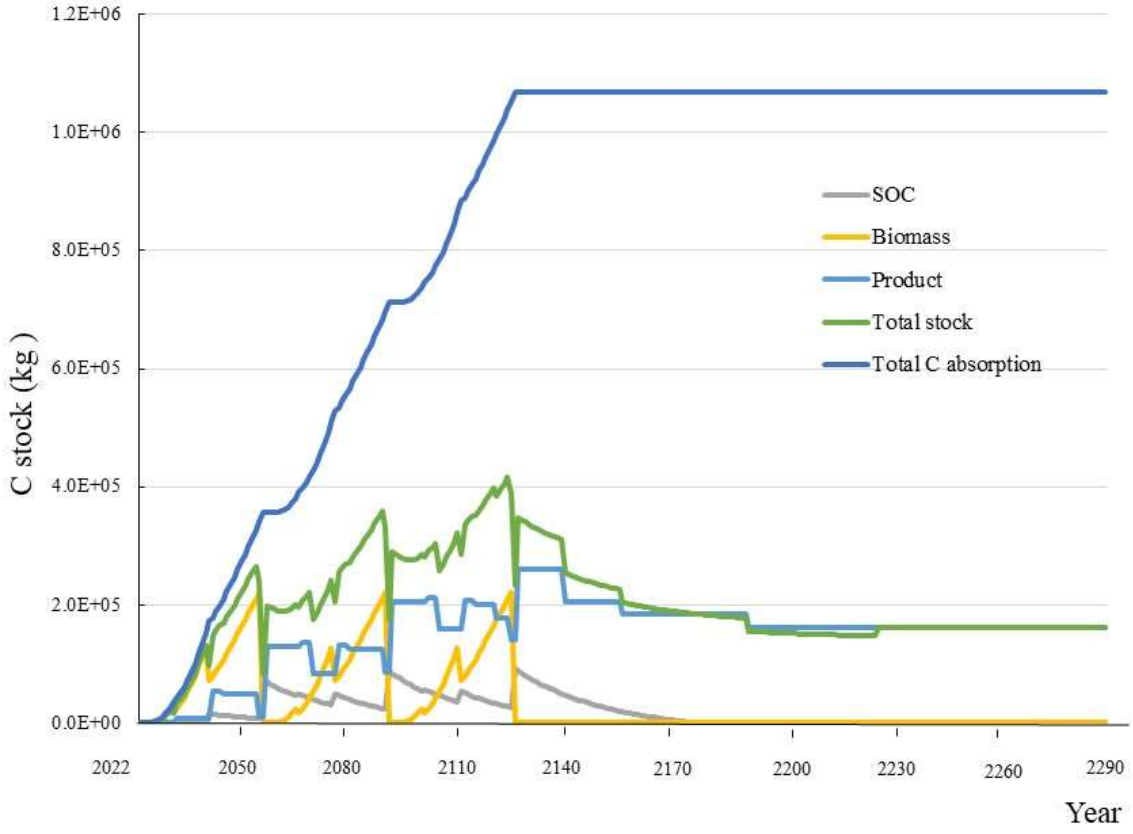

Fig. 11 Carbon captured over the cultivation period, and biogenic carbon stocks during the lifetime of the BL scenario.